

RESEARCH ARTICLE | MARCH 25 2024

Practical phase-space electronic Hamiltonians for *ab initio* dynamics FREE

Zhen Tao  ; Tian Qiu  ; Mansi Bhati  ; Xuezhi Bian  ; Titouan Duston  ; Jonathan Rawlinson  ; Robert G. Littlejohn  ; Joseph E. Subotnik 



J. Chem. Phys. 160, 124101 (2024)

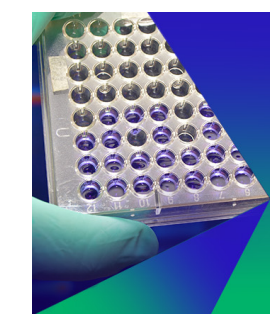
<https://doi.org/10.1063/5.0192084>



View
Online



Export
Citation



Biomicrofluidics

Special Topic:
Microfluidics and Nanofluidics in **India**

Submit Today



Practical phase-space electronic Hamiltonians for *ab initio* dynamics

Cite as: J. Chem. Phys. 160, 124101 (2024); doi: 10.1063/5.0192084

Submitted: 18 December 2023 • Accepted: 14 February 2024 •

Published Online: 25 March 2024



View Online



Export Citation



CrossMark

Zhen Tao,^{1,a)} Tian Qiu,¹ Mansi Bhati,¹ Xuezhi Bian,¹ Titouan Duston,¹ Jonathan Rawlinson,² Robert G. Littlejohn,³ and Joseph E. Subotnik^{1,b)}

AFFILIATIONS

¹ Department of Chemistry, University of Pennsylvania, Philadelphia, Pennsylvania 19104, USA

² Department of Mathematics, University of Manchester, Manchester M13 9PL, United Kingdom

³ Department of Physics, University of California, Berkeley, California 94720, USA

^{a)}Author to whom correspondence should be addressed: taozhen@sas.upenn.edu

^{b)}E-mail: subotnik@sas.upenn.edu

ABSTRACT

Modern electronic structure theory is built around the Born–Oppenheimer approximation and the construction of an electronic Hamiltonian $\hat{H}_{el}(\mathbf{X})$ that depends on the nuclear position \mathbf{X} (and not the nuclear momentum \mathbf{P}). In this article, using the well-known theory of electron translation (Γ') and rotational (Γ'') factors to couple electronic transitions to nuclear motion, we construct a practical phase-space electronic Hamiltonian that depends on both nuclear position and momentum, $\hat{H}_{PS}(\mathbf{X}, \mathbf{P})$. While classical Born–Oppenheimer dynamics that run along the eigensurfaces of the operator $\hat{H}_{el}(\mathbf{X})$ can recover many nuclear properties correctly, we present some evidence that motion along the eigensurfaces of $\hat{H}_{PS}(\mathbf{X}, \mathbf{P})$ can better capture both nuclear *and* electronic properties (including the elusive electronic momentum studied by Nafie). Moreover, only the latter (as opposed to the former) conserves the *total* linear and angular momentum in general.

Published under an exclusive license by AIP Publishing. <https://doi.org/10.1063/5.0192084>

I. INTRODUCTION

Born–Oppenheimer (BO) theory¹ is the workhorse of molecular dynamics.^{2–6} The basic premise is that one separates the slow nuclear degrees of freedom (\mathbf{X}) from the fast electronic degrees of freedom (\mathbf{r}). Mathematically, one decomposes the total Hamiltonian (nuclear + electronic, \hat{H}_{tot}) into the nuclear kinetic energy operator $\hat{T}_n(\mathbf{P})$ and the non-relativistic electronic Hamiltonian $\hat{H}_e(\mathbf{X})$,

$$\hat{H}_{tot} = \hat{T}_n(\mathbf{P}) + \hat{H}_e(\mathbf{X}). \quad (1)$$

For the moment, we ignore external fields. If one is running classical BO dynamics, one then diagonalizes the resulting electronic Hamiltonian,

$$\hat{H}_e(\mathbf{X})|\Phi_I(\mathbf{X})\rangle = E_I(\mathbf{X})|\Phi_I(\mathbf{X})\rangle, \quad (2)$$

and propagates Newton's equations along the eigensurface $E_I(\mathbf{X})$,

$$\dot{\mathbf{X}} = \frac{\mathbf{P}}{M}, \quad (3)$$

$$\dot{\mathbf{P}} = -\frac{\partial E_I}{\partial \mathbf{X}}. \quad (4)$$

Here, our notation is as follows. We label all electronic operators (or more generally matrices) with a hat, **boldface** indicated vectors in three-dimensional space, and we index all standard adiabatic states by I, J, K, \dots . Atomic orbitals (AO) are indexed below by $\{\mu, v, \lambda, \sigma\}$. The nuclei are indexed below by A, B, C, Q , and the Cartesian xyz are indexed by $\alpha\beta\gamma\kappa\eta$.

The Hamiltonian dynamics in Eqs. (1)–(4) conserve the total energy, the nuclear linear momentum, and the nuclear angular momentum. However, as demonstrated recently, these calculations do not conserve the *total* linear or angular momentum in general.⁷ One can easily reach this conclusion by imagining that we run BO dynamics along one doublet surface, here as constructed for a system with an odd number of electrons and spin-orbit coupling (SOC). In such a case, the electronic wavefunction becomes complex-valued and it is clear that the electronic linear and angular momentum of a given state will be nonzero, changing as a function of time. However,

Eqs. (1)–(4) will conserve only the nuclear angular momentum; thus, the *total* angular momentum must change as a function of time.

Given that the total angular momentum operator is strictly diagonal in the BO representation and should formally be conserved if one runs quantum dynamics along a single BO surface with the correct phase conventions,⁸ the resolution of this paradox is that one must supplement Eq. (4) with the proper Berry force,⁷

$$\dot{\mathbf{P}} = -\frac{\partial E_I}{\partial \mathbf{X}} + \mathbf{F}_I^{\text{Berry}}, \quad (5)$$

$$\mathbf{F}_I^{\text{Berry}} = \boldsymbol{\Omega}_I \cdot \dot{\mathbf{X}}, \quad (6)$$

$$\boldsymbol{\Omega}_I = i\hbar \nabla_n \times \mathbf{d}_{II}, \quad (7)$$

where $\boldsymbol{\Omega}$ is the Abelian Berry curvature and $\mathbf{d}_{II} = \langle \Phi_I | \nabla_n | \Phi_I \rangle$ is the on-diagonal derivative coupling vector between the state I and itself. The quantity $A = i\hbar \mathbf{d}_{II}$ is also known as the Berry connection and it is non-zero for systems with odd number of electrons⁹ and SOC for which we have complex wavefunctions and Kramers' pairs. By including the Berry force in Eq. (5), one recovers total angular momentum conservation with classical nuclear dynamics.⁷

Unfortunately, however, including a Berry force has two pitfalls. (i) Computing a Berry force can be quite expensive numerically because the Berry curvature involves the derivative of a derivative coupling (i.e., a second derivative)—which must always be avoided in *ab initio* calculations whenever possible. Note that the calculation can be made simpler for the specific case of a ground state calculation where the tensor has been derived and implemented for a generalized Hartree–Fock (HF) ansatz,^{10,11} but, overall, it is certainly desirable to avoid the Berry curvature for excited state dynamics. (ii) For the case of a system with electronic degeneracy (i.e., Kramers doublet), the notion of a Berry force is tricky and somewhat arbitrary because one must arbitrarily pick one doublet (e.g., I) out of a pair (e.g., I, I'). One can avoid the second pitfall by running Ehrenfest (mean-field) dynamics,¹² calculating the electronic density matrix $\hat{\rho}$ over a set of states and, as prescribed by Takatsuka¹³ and then Krishna,¹⁴ including the non-Abelian curvature¹⁵ in the force,

$$\hat{\Omega}_{\text{nab}}^{BaC\beta} = \frac{\partial \hat{A}^{C\beta}}{\partial X_{Ba}} - \frac{\partial \hat{A}^{B\alpha}}{\partial X_{C\beta}} - \frac{i}{\hbar} [\hat{A}^{B\alpha}, \hat{A}^{C\beta}]. \quad (8)$$

In such a case, one never needs to pick an arbitrary surface within a Kramers' pair and one does recover total (linear and angular) momentum conservation.¹² Alas, however, computing the non-Abelian Berry curvature in Eq. (8) is even more expensive than computing the Abelian Berry curvature in Eq. (7), and hence, the method will likely need future approximations to be practical for large systems.

A. Phase-space electronic Hamiltonians

Now, apart from including a Berry force of any kind, an alternative means to conserve the total momentum is to work from the start with a phase-space electronic Hamiltonian that depends on both nuclear position and momentum, $\hat{H}_{\text{PS}}(\mathbf{X}, \mathbf{P})$,

$$\hat{H}_{\text{PS}}(\mathbf{X}, \mathbf{P}) = \frac{\mathbf{P}^2}{2M} - i\hbar \frac{\mathbf{P}}{M} \cdot \hat{\Gamma} + \hat{H}_{\text{el}}(\mathbf{X}), \quad (9)$$

Here, we emphasize that the nuclear momentum operator has been replaced by the classical momentum \mathbf{P} and $\hat{\Gamma}$ is a nuclear–electronic coupling to be determined.¹⁶ The most famous example of Eq. (9) is Shenvi's phase-space electronic Hamiltonian¹⁷ in an adiabatic electronic basis,

$$\hat{H}_{\text{Shenvi}}(\mathbf{X}, \mathbf{P}) = \frac{\mathbf{P}^2}{2M} - i\hbar \frac{\mathbf{P} \cdot \hat{\mathbf{d}}}{M} - \hbar^2 \frac{\hat{\mathbf{d}} \cdot \hat{\mathbf{d}}}{2M} + \hat{E}_{ad}(\mathbf{X}), \quad (10)$$

where \hat{E}_{ad} is the diagonal matrix of eigenvalues of $\hat{H}_{\text{el}}(\mathbf{X})$ and $\hat{\mathbf{d}}$ is the density matrix of derivative couplings, which couples different electronic states I, J , where

$$\mathbf{P} \cdot \hat{\mathbf{d}} = \sum_{A\alpha} P_{A\alpha} \hat{d}^{A\alpha}, \quad (11)$$

$$\hat{\mathbf{d}} \cdot \hat{\mathbf{d}} = \sum_{A\alpha} \hat{d}^{A\alpha} \hat{d}^{A\alpha}, \quad (12)$$

$$d_{IJ}^{A\alpha} = \left\langle \Phi_I \left| \frac{\partial}{\partial X_{A\alpha}} \right| \Phi_J \right\rangle. \quad (13)$$

As shown in Ref. 16, if we diagonalize $\hat{H}_{\text{Shenvi}}(\mathbf{X}, \mathbf{P})$ and run classical dynamics along the corresponding eigensurfaces (that depend on \mathbf{X} and \mathbf{P}), we will indeed conserve the total linear and angular momentum.

Alas, there are also problems with the Hamiltonian in Eq. (10), some conceptual and some practical. (i) First, one limitation arises in the case of degenerate states, e.g., doublets. In such a case, given the complex-valued nature of the SOC, one must arbitrarily choose two basis states ($|\Phi_I\rangle$ and $|\Phi_{I'}\rangle$) and two complex-valued phases for each state, which leads to an arbitrary $\hat{\mathbf{d}}$ in Eq. (10), which ultimately renders the phase-space Hamiltonian of limited value in such a case; the algorithm cannot be reliable for systems with electronic degeneracy, e.g., systems with odd numbers of electrons. (ii) A second limitation is numerical stability. Near a conical intersection, the derivative coupling $\hat{\mathbf{d}}$ will diverge, and one will recover spikes in the eigenenergies of $\hat{H}_{\text{Shenvi}}(\mathbf{X}, \mathbf{P})$ in Eq. (10).¹⁸ (iii) A third limitation is computational cost. For a number of N adiabatic states, the algorithm requires the computation of $N(N+1)/2$ numbers of derivative couplings to construct $\hat{H}_{\text{Shenvi}}(\mathbf{X}, \mathbf{P})$ in Eq. (10), and as discussed above, running dynamics on the potential energy surfaces requires the derivatives of those derivative couplings. For these reasons, as far as we are aware, no one has ever worked with the Hamiltonian in Eq. (10) for any *ab initio* calculations. Thus, it is desirable to approximate the derivative coupling vector while maintaining important features, such as momentum conservation.

B. Necessary conditions for linear and angular momentum conservation

Interestingly, to satisfy momentum conservation, Eq. (10) is not the only phase-space Hamiltonian. In fact, if at all one seeks momentum conservation, one does not need to compute $\hat{\mathbf{d}}$ necessarily. As discussed in Ref. 16 in the phase-space surface hopping context, if one works with a subspace of adiabatic states and introduces a $\Gamma_{IJ}^{A\alpha}$ matrix (in place of the derivative coupling), one can ensure momentum conservation as long as the following four conditions are satisfied:

$$-i\hbar \sum_A \Gamma_{IJ}^{A\alpha} + \langle \Phi_I | \hat{p}_e^\alpha | \Phi_J \rangle = 0, \quad (14)$$

$$\sum_B \nabla_{B\beta} \Gamma_{IJ}^{A\alpha} = 0, \quad (15)$$

$$-i\hbar \sum_{A\beta\gamma} \epsilon_{\alpha\beta\gamma} X_{A\beta} \Gamma_{IJ}^{A\gamma} + \langle \Phi_I | \hat{L}_e^\alpha + \hat{s}^\alpha | \Phi_J \rangle = 0, \quad (16)$$

$$\sum_{B\beta\eta} \epsilon_{\alpha\beta\eta} X_{B\beta} \nabla_{B\eta} \Gamma_{IJ}^{A\gamma} + \sum_\eta \epsilon_{\alpha\gamma\eta} \Gamma_{IJ}^{A\eta} = 0, \quad (17)$$

where $\epsilon_{\alpha\beta\gamma}$ is the Levi–Civita symbol. Below, we will write the matrix elements of the electronic linear momentum operator \hat{p}_e^α , the electronic orbital angular momentum operator \hat{L}_e^α and the electronic spin operator \hat{s}^α in AO basis as $p_{\mu\nu}^\alpha$, $l_{\mu\nu}^\alpha$, and $s_{\mu\nu}^\alpha$, respectively.

On the one hand, the conditions in Eqs. (14) and (16) are really phase conventions,⁸ i.e., the conventions for choosing the phases of the electronic states at different geometries. On the other hand, the conditions in Eqs. (15) and (17) ensure that the coupling transforms are invariant under translational and rotational changes of coordinate,

$$\Gamma_{IJ}^{A\alpha}(\mathbf{X}_0 + \delta\mathbf{X}) = \Gamma_{IJ}^{A\alpha}(\mathbf{X}_0), \quad (15')$$

$$\Gamma_{IJ}(\mathbf{R}\mathbf{X}_0) = \mathbf{R}\Gamma_{IJ}(\mathbf{X}_0), \quad (17')$$

where \mathbf{R} is the rotation operator in the Cartesian xyz space, $\mathbf{R} = \exp(-\frac{i}{\hbar} \sum_a \mathbf{L}^\alpha \delta_\alpha)$, and $L_{\beta\gamma}^\alpha = -i\hbar \epsilon_{\alpha\beta\gamma}$. As a side note, as shown in Ref. 16, the full derivative couplings $\hat{\mathbf{d}}$ do satisfy all four constraints [Eqs. (14)–(17)].

Now, with so many choices for Γ_{IJ} possible in order to conserve momentum, one must wonder what is the optimal path for building such a term. For practical purposes, one would prefer the simplest way possible. In particular, one would like to avoid the cumbersome process of diagonalizing the electronic Born–Oppenheimer Hamiltonian, generating states I and J , adding a momentum-dependent term $\mathbf{P} \cdot \Gamma_{IJ}$ in the spirit of Eqs. (1)–(4), rediagonalizing the resulting phase-space Hamiltonian, and then generating gradients for dynamics. Such a multi-step approach is not very practical.

C. Outline of this paper

The goal of this paper is to provide an alternative, one-shot treatment for generating phase-space Hamiltonians with Γ -couplings. More precisely, we will derive and implement a meaningful Γ matrix that arises from a one-electron operator so that, at the end of the day, we need only to diagonalize a single electronic Hamiltonian, and motion along the resulting surfaces will automatically conserve momentum while also being very efficient.

To that end, in Sec. II below, we will show that Eqs. (14)–(17) for Γ_{IJ} can indeed be satisfied for a proper one-electron operator $\Gamma_{\mu\nu} a_\mu^\dagger a_\nu$ in an atomic orbital basis, $\Gamma_{IJ} = \sum_{\mu\nu} \langle \Phi_I | \Gamma_{\mu\nu} a_\mu^\dagger a_\nu | \Phi_J \rangle$, and we will delineate the necessary conditions for $\Gamma_{\mu\nu}$ in order to conserve linear and angular momentum. Next, with so many possible choices for Γ , in Sec. III, we will posit that one means for isolating a physically meaningful one-electron operator $\Gamma_{\mu\nu}$ is to insist that the phase-space electronic Hamiltonian should yield the correct expression for linear (and sometimes angular) momentum (which requires a beyond Born–Oppenheimer calculations as developed by Nafie^{19–22}). Finally, in Sec. IV, we provide results, demonstrating

both the size of the relevant matrix elements as well as the capacity of the resulting method to recapitulate electronic momentum and angular momentum. In Sec. VI, we discuss the future implications of this work and conclude.

II. THEORY: A STABLE ANSATZ FOR A ONE-ELECTRON HAMILTONIAN OPERATOR $\Gamma_{\mu\nu}$

While Eqs. (14)–(17) dictate the form of Γ_{IJ} in a many-body basis, the relevant conditions required of a single electron operator $\Gamma_{\mu\nu}$ are slightly different because the orientation of each atomic orbital is always fixed in the lab frame and does not rotate with the molecule. In other words, for example, for a rotation molecule, a p_x orbital is always polarized in the x –direction. Nevertheless, we will show below that if the following conditions are obeyed:

$$-i\hbar \sum_A \Gamma_{\mu\nu}^{A\alpha} + p_{\mu\nu}^\alpha = 0, \quad (18)$$

$$\sum_B \nabla_{B\beta} \Gamma_{\mu\nu}^{A\alpha} = 0, \quad (19)$$

$$-i\hbar \sum_{A\beta\gamma} \epsilon_{\alpha\beta\gamma} X_{A\beta} \Gamma_{\mu\nu}^{A\gamma} + l_{\mu\nu}^\alpha + s_{\mu\nu}^\alpha = 0, \quad (20)$$

$$\sum_{B\beta\eta} \epsilon_{\alpha\beta\eta} X_{B\beta} \langle \mu | \frac{\partial \hat{\Gamma}^{A\gamma}}{\partial X_{B\eta}} | v \rangle - \frac{i}{\hbar} \langle \mu | [\hat{\Gamma}^{A\gamma}, \hat{L}_e^\alpha] | v \rangle + \sum_\eta \epsilon_{\alpha\gamma\eta} \Gamma_{\mu\nu}^{A\eta} = 0, \quad (21)$$

then the linear and angular momentum will be conserved. Similar to the many-body case above, we note that Eqs. (19) and (21) are equivalent to

$$\Gamma_{\mu\nu}^{A\alpha}(\mathbf{X}_0 + \delta\mathbf{X}) = \Gamma_{\mu\nu}^{A\alpha}(\mathbf{X}_0), \quad (19')$$

$$\Gamma_{\bar{\mu}\bar{\nu}}(\mathbf{R}\mathbf{X}_0) = \mathbf{R}\Gamma_{\mu\nu}(\mathbf{X}_0). \quad (21')$$

Here, a word about notation and basis set definition is essential. If $|v\rangle$ is centered on atom B , and the molecule is rotated by an amount δ , then here we define the atomic orbital $|\bar{v}\rangle$ in Eq. (21') to be that orbital generated by rotation around atom B by the same rotational angle, $|\bar{v}_B\rangle \equiv \exp(-\frac{i}{\hbar} \sum_a \hat{L}_e^{Ba} \delta_a) |v_B\rangle$. As mentioned above, the fact that atomic orbitals are defined in a lab frame (rather than molecular frame) within quantum chemistry codes leads to the differences between Eqs. (21) and (21') with Eqs. (17) and (17') above (where the indices of $\Gamma(\mathbf{R}\mathbf{X}_0)$ are $\bar{\mu}, \bar{\nu}$ instead of μ, ν). The equivalence between Eqs. (21') and (21) for a general one-electron operator is shown in Appendix A.

A. Equations of motion

Let us now prove the claims above about momentum conservation. We begin by writing the total energy of the phase-space Hamiltonian for a single state in an atomic orbital basis,

$$E_{PS}(X, P) = \frac{P^2}{2M} + \sum_{\mu\nu} D_{\nu\mu} \left(h_{\mu\nu} - i\hbar \sum_{A\alpha} \frac{P_{A\alpha} \Gamma_{\mu\nu}^{A\alpha}}{M^A} \right) + \sum_{\mu\nu\lambda\sigma} G_{\nu\mu\lambda\sigma} \pi_{\mu\nu\lambda\sigma}, \quad (22)$$

where the quantities $D_{\nu\mu}$ and $G_{\nu\mu\lambda\sigma}$ are the one-electron and two-electron density matrix elements obtained from solving the phase-space Hamiltonian directly, respectively. The $h_{\mu\nu}$ and $\pi_{\mu\nu\lambda\sigma}$ matrix

elements are the relevant one-electron and two-electron operators in the atomic orbital basis. Given this energy expression, we can write the classical equations of motion to propagate the phase-space variables (\mathbf{X}, \mathbf{P}),

$$\dot{X}_{A\alpha} = \frac{P_{A\alpha}}{M^A} - i\hbar \sum_{\mu\nu} \frac{D_{\nu\mu} \Gamma_{\mu\nu}^{A\alpha}}{M^A}, \quad (23)$$

$$\dot{P}_{A\alpha} = -\frac{\partial E_{PS}}{\partial X_{A\alpha}} \quad (24)$$

$$= -\sum_{\mu\nu} D_{\nu\mu} \left(\frac{\partial h_{\mu\nu}}{\partial X_{A\alpha}} - \sum_{B\beta} \frac{i\hbar P_{B\beta}}{M^B} \frac{\partial \Gamma_{\mu\nu}^{B\beta}}{\partial X_{A\alpha}} \right) \\ - \sum_{\mu\nu\lambda\sigma} G_{\mu\nu\lambda\sigma} \frac{\partial \pi_{\mu\nu\lambda\sigma}}{\partial X_{A\alpha}} + \sum_{\mu\nu} W_{\nu\mu} \frac{\partial S_{\mu\nu}}{\partial X_{A\alpha}}, \quad (25)$$

where the S matrix is the overlap matrix and W is the energy-weighted density matrix. In going from Eqs. (24) to (25), we avoid the expensive step of calculating the orbital dependence on the nuclear positions according to Wigner's $(2n+1)$ rule (which is well-known in quantum chemistry).^{23,24} Now, let us examine the momentum conservation laws.

B. Linear momentum

For the case of linear momentum conservation, using Eq. (23), one evaluates

$$\frac{d}{dt} P_{tot}^\alpha = \frac{d}{dt} \left(\sum_A M_A \dot{X}_{A\alpha} + \sum_{\mu\nu} D_{\nu\mu} P_{\mu\nu}^\alpha \right) \quad (26)$$

$$= \frac{d}{dt} \left[\sum_A P_{A\alpha} + \sum_{\mu\nu} D_{\nu\mu} \left(\sum_A -i\hbar \Gamma_{\mu\nu}^{A\alpha} + p_{\mu\nu}^\alpha \right) \right]. \quad (27)$$

Now, if we plug Eq. (18) into Eq. (27), the second term on the right-hand side (RHS) vanishes, and we can simplify

$$\frac{d}{dt} P_{tot}^\alpha = \sum_A \dot{P}_{A\alpha} = -\sum_A \frac{\partial E_{PS}}{\partial X_{A\alpha}}. \quad (28)$$

From Eq. (28), one concludes that in order for the total linear momentum to conserve ($\frac{d}{dt} P_{tot}^\alpha = 0$), the phase-space energy needs to be translationally invariant ($\sum_A \frac{\partial E_{PS}}{\partial X_{A\alpha}} = 0$). If we dig a little deeper and plug Eq. (25) into Eq. (28), we find

$$\frac{d}{dt} P_{tot}^\alpha = i\hbar \sum_{B\beta\mu\nu} \frac{P_{B\beta}}{M^B} D_{\nu\mu} \sum_A \frac{\partial \Gamma_{\mu\nu}^{B\beta}}{\partial X_{A\alpha}}. \quad (29)$$

Note that, in Eq. (29), we have already excluded the relevant $h_{\mu\nu}$, $\pi_{\mu\nu\lambda\sigma}$, and $S_{\mu\nu}$ terms from the gradient because these matrices are translation-invariant, i.e., $\sum_A \frac{\partial h_{\mu\nu}}{\partial X_{A\alpha}} = 0$, $\sum_A \frac{\partial \pi_{\mu\nu\lambda\sigma}}{\partial X_{A\alpha}} = 0$, and $\sum_A \frac{\partial S_{\mu\nu}}{\partial X_{A\alpha}} = 0$. Finally, we conclude that according to Eqs. (19) and (29), $\dot{P}_{tot}^\alpha = 0$. Thus, conditions Eqs. (18) and (19) are sufficient to guarantee linear momentum conservation.

C. Angular momentum

Next, we evaluate the angular momentum,

$$\frac{d}{dt} L_{tot}^\alpha = \frac{d}{dt} \left[\sum_{A\beta\gamma} \epsilon_{\alpha\beta\gamma} X_{A\beta} M_A \dot{X}_{A\gamma} + \sum_{\mu\nu} (l_{\mu\nu}^\alpha + s_{\mu\nu}^\alpha) D_{\nu\mu} \right] \quad (30)$$

$$= \frac{d}{dt} \left[\sum_{A\beta\gamma} \epsilon_{\alpha\beta\gamma} X_{A\beta} P_{A\gamma} + \sum_{A\mu\nu\beta\gamma} (-i\hbar \epsilon_{\alpha\beta\gamma} X_{A\beta} \Gamma_{\mu\nu}^{A\gamma} + l_{\mu\nu}^\alpha + s_{\mu\nu}^\alpha) D_{\nu\mu} \right]. \quad (31)$$

If we plug Eq. (20) into Eq. (31) to eliminate the second term on the RHS of Eq. (31), we are left with

$$\frac{d}{dt} L_{tot}^\alpha = \sum_{A\beta\gamma} \epsilon_{\alpha\beta\gamma} (\dot{X}_{A\beta} P_{A\gamma} + X_{A\beta} \dot{P}_{A\gamma}) \quad (32)$$

$$= -\sum_{A\beta\gamma} \epsilon_{\alpha\beta\gamma} \left(P_{A\beta} \frac{\partial E_{PS}}{\partial P_{A\gamma}} + X_{A\beta} \frac{\partial E_{PS}}{\partial X_{A\gamma}} \right). \quad (33)$$

From Eq. (33), it follows (not surprisingly) that in order for the total angular momentum to be conserved, the energy of the phase-space electronic Hamiltonian must be rotationally invariant. Mathematically, requiring a vanishing RHS of Eq. (33) is equivalent to requiring the energy $E_{PS}(\mathbf{X}, \mathbf{P})$ in Eq. (22) to satisfy

$$E_{PS}(RX, RP) = E_{PS}(X, P). \quad (34)$$

Let us now evaluate all of the terms in Eq. (22) individually. To begin with, one can immediately see that the nuclear kinetic energy is rotationally invariant because $\mathbf{P}^2 = \mathbf{RP} \cdot \mathbf{RP}$. For the remaining contributions in Eq. (22), we recall that the one-electron and two-electron operators written in the atomic orbital basis satisfy

$$h_{\bar{\mu}\bar{\nu}}(RX_0) = h_{\mu\nu}(X_0), \quad (35)$$

$$\pi_{\bar{\mu}\bar{\nu}\bar{\lambda}\bar{\sigma}}(RX_0) = \pi_{\mu\nu\lambda\sigma}(X_0). \quad (36)$$

Equations (35) and (36) are proven in Appendix A. Here, if we rotate the molecule by a rotation R , we also imagine rotating all of shells of basis functions around each atomic center by the corresponding unitary matrix $\hat{U}(X)$ to generate rotated basis functions. In other words, if $|\bar{v}\rangle \in S$, for a specific shell (S), we define: $|\bar{v}\rangle = \sum_{v \in S} |v\rangle U_{\bar{v}}$.

Finally, as far as the Γ matrix is concerned, according to Eq. (21'), we know that

$$RP \cdot \Gamma_{\bar{\mu}\bar{\nu}}^A(RX_0) = RP \cdot R\Gamma_{\mu\nu}^A(X_0) = P \cdot \Gamma_{\mu\nu}^A(X_0). \quad (37)$$

Therefore, at the end of the day, all of the matrix elements within the energy expression E_{PS} from Eq. (22) are rotationally invariant, and it follows from a variational treatment that the one- and two-electron density matrices must also be rotationally invariant [$D_{\bar{\mu}\bar{\nu}}(RX_0) = D_{\mu\nu}(X_0)$, $G_{\bar{\mu}\bar{\nu}\bar{\lambda}\bar{\sigma}}(RX_0) = G_{\mu\nu\lambda\sigma}(X_0)$]. Thus, we may conclude that, so long as the Γ matrix satisfies the four conditions given in Eqs. (18)–(21'), the energy E_{PS} will also be rotationally invariant and satisfy Eq. (34).

D. An ansatz for Γ from the theory of electron translation and rotation factors²⁵

For a practitioner of surface hopping dynamics,^{3,26–28} one immediately recognizes the constraints in Eqs. (18)–(21'), as these are the constraints that guide the construction of electron translation factors (ETFs)²⁹ and electron rotation factors (ERFs),³⁰ which are discussed in a companion paper (Ref. 25). See Eqs. (15), (16), (A5), and (B18) in Ref. 25. To that end, some words of background are appropriate here.

During the course of a surface hopping trajectory, it is well established from model studies^{31–34} that, when hopping from state I to state J , the nuclear momentum should be rescaled in the direction of the derivative coupling vector \mathbf{d}_{IJ} in order to conserve energy (and establish a balance between kinetic and potential energy). However, from a mathematical point of view, this momentum rescaling scheme changes the total momentum because the derivative couplings satisfy

$$-i\hbar \sum_A d_{IJ}^{A\alpha} = -\langle \Phi_I | \hat{p}_e^\alpha | \Phi_J \rangle, \quad (38)$$

$$-i\hbar \sum_{A\beta\gamma} \epsilon_{\alpha\beta\gamma} X^{A\beta} d_{IJ}^{A\gamma} = -\langle \Phi_I | \hat{L}_e^\alpha + \hat{s}^\alpha | \Phi_J \rangle. \quad (39)$$

The above equations for \mathbf{d}_{IJ} are exactly the same as Eqs. (14) and (16) for the Γ_{IJ} coupling and reflect a phase convention for the electronic states $|\Phi_I\rangle$ and $|\Phi_J\rangle$.⁸ From a physical point of view, the RHS of Eqs. (39) and (38) is nonzero because whenever the nuclei move along one adiabatic state, that motion also drags around electrons. Thus, whenever the molecular nuclei are translated and/or rotated, that motion can induce changes in electronic linear and/or angular momentum and eventually lead to an electronic transition.

Now, the fact that rescaling along the derivative coupling direction destroys the conservation of *nuclear* linear and angular momentum has long bothered chemists.^{16,30,35} For the most part, chemists have regarded this failure as a limitation of semiclassical mechanics and the desire has always been to fix this problem by restoring the linear and angular momentum of the nuclei in some fashion or another.^{25,29,30,35} To that end, in Refs. 29 and 30, in order to restore nuclear momentum conservation, we previously sought to remove the offending translational and rotational components of the derivative coupling, i.e., which leads to the notion of ETFs and ERFs, respectively.

1. Electronic translation factors

We begin with ETFs. ETFs restore linear momentum conservation and can be isolated by working on a translating basis.^{36–42} As a practical matter, constructing an ETF to restore linear momentum conservation is quite trivial from an electronic structure point of view: in any AO basis, whether for multireference configuration interaction (MRCI)^{43–45} or configuration interaction singles (CIS)²⁹ or time-dependent density functional theory (approximate)^{46–52} wavefunctions, one always finds that the derivative coupling vector between states I and J naturally decomposes into

$$\mathbf{d}_{IJ}^{tot} = \mathbf{d}_{IJ}^{ETF} + \tilde{\mathbf{d}}_{IJ}^0, \quad (40)$$

where \mathbf{d}_{IJ}^{ETF} is effectively the matrix element for the one-electron momentum operator,

$$d_{IJ}^{ETF,A\alpha} = \sum_{\mu\nu} \left\langle I | \Gamma'_{\mu\nu}^{A\alpha} a_\mu^\dagger a_\nu | J \right\rangle, \quad (41)$$

$$\Gamma'_{\mu\nu}^{A\alpha} = \frac{1}{2i\hbar} p_{\mu\nu}^\alpha (\delta_{BA} + \delta_{CA}). \quad (42)$$

Here, in Eq. (42), we assume $|\mu\rangle$ is centered on atom B and $|\nu\rangle$ is centered on atom C. Mathematically, Γ' in Eq. (42) clearly satisfies Eqs. (18) and (19).

On a very practical note, $\tilde{\mathbf{d}}_{IJ}^0$ is what remains after subtracting away the ETF component and it is straightforward to separate d_{IJ}^{ETF} from $\tilde{\mathbf{d}}_{IJ}^0$ because the latter scales like $1/(E_I - E_J)$ and blows up around a conical intersection; the former does not.

2. Electronic rotation factors

Next, we consider ERFs; altogether, a combination of ETFs and ERFs should restore linear and angular momentum. Now, while ERFs are rarely discussed in the literature (as compared with ETFs), by working on a basis that both translates and rotates, we have recently shown that one can indeed construct ERFs.^{25,30} Thus, one can decompose the total derivative coupling into three parts: an ETF part, an ERF part of the derivative coupling vector, and the remaining part

$$\mathbf{d}_{IJ}^{tot} = \mathbf{d}_{IJ}^{ETF} + \mathbf{d}_{IJ}^{ERF} + \mathbf{d}_{IJ}^0, \quad (43)$$

where

$$d_{IJ}^{ERF,A\alpha} = \sum_{\mu\nu} \left\langle \Phi_I | \Gamma''_{\mu\nu}^{A\alpha} a_\mu^\dagger a_\nu | \Phi_J \right\rangle. \quad (44)$$

Here, the form of Γ'' is necessarily more complicated than the form for Γ' because the latter can be a local one-electron operator and the former only a semi-local one-electron operator.^{25,30} Using the same atom labels (A,B,C) as above for the ETFs [Eq. (42)], according to Ref. 25, one reasonable form for Γ'' is²⁵

$$\Gamma''_{\mu\nu}^{A\alpha} = \zeta_{\mu\nu}^A (X_A - X_{\mu\nu}^0) \times (K_{\mu\nu}^{-1} J_{\mu\nu}), \quad (45)$$

where

$$J_{\mu\nu} = \frac{1}{i\hbar} \left\langle \mu \left| \frac{1}{2} (\hat{L}_e^B + \hat{L}_e^C) \right| \nu \right\rangle, \quad (46)$$

$$\zeta_{\mu\nu}^A = \exp \left(-w \frac{2|(X_A - X_B)|^2 |(X_A - X_C)|^2}{|(X_A - X_B)|^2 + |(X_A - X_C)|^2} \right), \quad (47)$$

$$X_{\mu\nu}^0 = \sum_A \zeta_{\mu\nu}^A X_A / \sum_A \zeta_{\mu\nu}^A, \quad (48)$$

$$\begin{aligned} K_{\mu\nu} = & - \sum_A \zeta_{\mu\nu}^A (X_A - X_{\mu\nu}^0)^\top (X_A - X_{\mu\nu}^0) \mathcal{I}_3 \\ & + \sum_A \zeta_{\mu\nu}^A (X_A - X_{\mu\nu}^0) (X_A - X_{\mu\nu}^0)^\top. \end{aligned} \quad (49)$$

Here, \mathcal{I}_3 is a 3×3 identity matrix. The parameter w here controls the locality, and in Ref. 25, 0.3 bohr⁻² was found to be a safe choice. See the discussion below for the importance of locality for

ERF. The definition of one of the Cartesian components (η) of \hat{L}_e^B in Eq. (46) is

$$\hat{L}_e^{B\eta} = [(\hat{\mathbf{r}}_e - \mathbf{X}_B) \times \hat{\mathbf{p}}_e]_\eta = \hat{L}_e^\eta - \sum_{\beta\gamma} e_{\eta\beta\gamma} X_{B\beta} \hat{p}_e^\gamma. \quad (50)$$

Although slightly more involved, it can be proven²⁵ that the one-electron matrix elements,

$$\Gamma_{\mu\nu} = \Gamma'_{\mu\nu} + \Gamma''_{\mu\nu}, \quad (51)$$

satisfy both Eqs. (18) and (20) above. Finally, as shown in Ref. 25, the ETF + ERF matrix $\Gamma_{\mu\nu}$ transforms correctly under translations and rotations of the molecule. In particular, Eqs. (A5) and (B18) in Ref. 25 are identical with Eqs. (19) and (21') above.

3. A phase-space Hamiltonian that approximates Eq. (10)

At the end of the day, choosing the Γ -couplings in Eq. (9) to be the ETFs + ERFs from Ref. 25 makes a great deal of sense. In short, rather than removing out the $\hat{\mathbf{d}}_{ETF}$ and $\hat{\mathbf{d}}_{ERF}$ vectors and rescaling along the $\hat{\mathbf{d}}_0$ direction within a standard surface hopping calculation, we imagine including explicit momentum coupling to the $\hat{\mathbf{d}}_{ETF}$ and $\hat{\mathbf{d}}_{ERF}$ vectors within a phase-space electronic Hamiltonian. Heuristically, this choice can be rationalized by rewriting Eq. (10) above as

$$\hat{H}_{Shenvi}(\mathbf{X}, \mathbf{P}) = \frac{\mathbf{P}^2}{2M} - i\hbar \frac{\mathbf{P} \cdot (\hat{\mathbf{d}}_{ETF} + \hat{\mathbf{d}}_{ERF} + \hat{\mathbf{d}}_0)}{M} - \hbar^2 \frac{\hat{\mathbf{d}} \cdot \hat{\mathbf{d}}}{2M} + \hat{E}_{ad}(\mathbf{X}). \quad (52)$$

Our recommended choice of the phase-space electronic Hamiltonian [using Eqs. (9), (42), (45), and (51) above] is equivalent to removing the $\mathbf{P} \cdot \hat{\mathbf{d}}_0$ term (which is gauge-dependent and explodes in the vicinity of avoided crossings but vanishes far from crossings) as well as the $\hat{\mathbf{d}} \cdot \hat{\mathbf{d}}$ term (which is often neglected in an \hbar expansion) in Eq. (52).

III. THE MISSING INGREDIENT: ELECTRONIC MOMENTUM

We have made the hypothesis above that a meaningful choice for Γ in Eq. (9) is to set these couplings equal to the sum of the ETFs and ERFs in Eqs. (42) and (45). One means of judging the value of such an ansatz for couplings is to compare the resulting predictions for electronic momentum vis a vis Nafie's celebrated expression^{19–22} for electronic momentum. At this point, a brief interlude (and review) of Nafie's work is appropriate.

To begin our review, note that one obvious failure of the BO approximation is the fact that motion along an adiabatic surface does not carry any electronic momentum.^{53–56} Mathematically, for any electronic wavefunction $|\Phi_I\rangle$ constructed by Eq. (2), $\langle\Phi_I|\hat{\mathbf{p}}_e|\Phi_I\rangle = 0$. This failure can be addressed by going to a higher order in BO theory,^{40,57–65} and identifying either the momentum or the electronic

flux.^{66–68} Mathematically, if we regard the term $-i\hbar \frac{\mathbf{P} \cdot \hat{\mathbf{d}}}{M}$ as the perturbation in Eq. (10), one can construct the perturbed wavefunction as follows (by summing over all other electronic state J):

$$|\Psi_I\rangle = |\Phi_I\rangle - i\hbar \sum_{J \neq I} \frac{\langle\Phi_J|\sum_A \frac{\mathbf{P}^A \cdot \hat{\mathbf{d}}^A}{M_A}|\Phi_I\rangle}{E_I - E_J} |\Phi_J\rangle, \quad (53)$$

where $\langle\Phi_I|\hat{\mathbf{d}}^A|\Phi_J\rangle \equiv \mathbf{d}_{IJ}^A$. We can now evaluate the expectation value of $\langle\Psi_I|\hat{\mathbf{p}}_e|\Psi_I\rangle$,

$$\langle\Psi_I|\hat{\mathbf{p}}_e|\Psi_I\rangle = 2\hbar \text{Im} \sum_{J \neq I} \frac{\langle\Phi_J|\sum_A \frac{\mathbf{P}^A \cdot \hat{\mathbf{d}}^A}{M_A}|\Phi_I\rangle}{E_I - E_J} \langle\Phi_I|\hat{\mathbf{p}}_e|\Phi_J\rangle. \quad (54)$$

At this point, let us assume a complete basis, restrict ourselves to the case of no spin-orbit coupling, and use the commutator,

$$[\hat{H}_e, \hat{\mathbf{r}}_e] = -i\hbar \frac{\hat{\mathbf{p}}_e}{m_e}. \quad (55)$$

From this exact relationship, it follows that:

$$(E_I - E_J)\langle\Phi_I|\hat{\mathbf{r}}_e|\Phi_J\rangle = -i\hbar \frac{1}{m_e} \langle\Phi_I|\hat{\mathbf{p}}_e|\Phi_J\rangle. \quad (56)$$

Then, if we plug Eq. (56) into Eq. (54) and use the fact that $\langle\Phi_I|\hat{\mathbf{d}}^A|\Phi_I\rangle = 0$, we find

$$\langle\Psi_I|\hat{\mathbf{p}}_e|\Psi_I\rangle = 2m_e \text{Re} \sum_J \left\langle\Phi_J \left| \sum_A \frac{\mathbf{P}^A \cdot \hat{\mathbf{d}}^A}{M_A} \right| \Phi_I\right\rangle \langle\Phi_I|\hat{\mathbf{r}}_e|\Phi_J\rangle \quad (57)$$

$$= 2m_e \text{Re} \left\langle\Phi_I \left| \hat{\mathbf{r}}_e \sum_A \frac{\mathbf{P}^A \cdot \hat{\mathbf{d}}^A}{M_A} \right| \Phi_I\right\rangle \quad (58)$$

$$= 2m_e \text{Re} \left\langle\Phi_I \left| \hat{\mathbf{r}}_e \frac{d}{dt} \Phi_I \right| \Phi_I\right\rangle, \quad (59)$$

$$\langle\Psi_I|\hat{\mathbf{p}}_e|\Psi_I\rangle = m_e \frac{d}{dt} \langle\Phi_I|\hat{\mathbf{r}}_e|\Phi_I\rangle. \quad (60)$$

Equation (60) is Nafie's celebrated final result for the electronic momentum. Clearly, Eq. (60) should be satisfied (or approximately satisfied) with a meaningful choice of Γ . In the extremely well-separated adiabatic limit, where there are minimal nonadiabatic interactions, this expression is the physical electronic momentum. One means of checking the validity of any choice of $\Gamma_{\mu\nu}$ [with the corresponding phase-space Hamiltonian in Eq. (9)] is to evaluate the electronic momentum and see whether or not the result satisfies Eq. (60).

As a side note, we mention that Eq. (60) is valid in the adiabatic limit, i.e., when moving along a well-separated adiabat E_I . If one performs a nonadiabatic simulation and wishes to estimate the electronic momentum from a collection of states using a complete basis and a full CI Hamiltonian, one can derive a proper expression for the electronic momentum by using the corresponding electronic density matrix; as shown by Takatsuka,⁶⁷ one can even check the validity of the continuity equation for the electronic momentum probability density in a finite basis. Our hope for the present electronic phase-space Hamiltonian is that one will be able to compute electronic momenta from a single adiabatic state calculation (as opposed to a full nonadiabatic calculation) in the adiabatic limit.

A. Beyond Nafie: The search for electronic angular momentum

Beyond linear momentum, we would also very much like a means to benchmark the predicted electronic angular momentum as well. Unfortunately, however, the approach from the previous section cannot be generalized to the case of angular momentum and there is no simple final expression [as in Eq. (60)] for $\langle \Psi_I | \hat{L}_e | \Psi_I \rangle$. The reason is simple: While Eq. (60) above is the quantum mechanical analog of the classical expression, $p_e = m_e \frac{dr_e}{dt}$, there is no analogous expression for rotations. For a simple rotation in two dimensions, one can write $L = \mathcal{I} \frac{d\theta}{dt}$, where L is the angular momentum, \mathcal{I} is the moment of inertia, and θ is the relevant angle; however, for a multi-dimensional problem, there is no unique θ and \mathcal{I} becomes a matrix. Mathematically, one big issue is commutativity: whereas \hat{p}_e^x and \hat{p}_e^y commute, \hat{L}_e^x and \hat{L}_e^y do not commute, and this lack of commutativity prevents any multidimensional analog of Eq. (60) for angular momentum. Thus, in principle, if one wishes to estimate the electronic angular momentum, one needs to evaluate a full sum over states as in Eq. (54), which is indeed painful.

Nevertheless, in the limit of the two-dimensional motion of a rigid linear (or linear like) molecule in the xy plane, the algorithm above can be partially adapted by recognizing that the relevant quantum mechanical expression is

$$\hat{H} = -\frac{\hbar^2}{2m_e r_e^2} \frac{\partial^2}{\partial \theta^2} = \frac{\hat{L}_e^2}{2m_e r_e^2}, \quad (61)$$

$$[\hat{H}, m_e r_e^2 \hat{\theta}] = -i\hbar \cdot \hat{L}_e. \quad (62)$$

Here, we transform to relative coordinates, assume the center of mass is placed at the origin, and define $r_e^2 = x^2 + y^2$ as the distance of the particle away from the origin.

TABLE I. The α components of the linear momentum (\hbar/a_0) calculated with a translational velocity along the α axis. The linear molecules are aligned along the x axis, and we report translations for the $\alpha = x, y$ directions. The finite-difference (FD) approach in Eq. (60) serves as the benchmark and does not change with different basis sets. The linear momentum calculated with the phase-space Hamiltonian approaches the finite-difference values for larger basis sets.

| | STO-3G | DZ | aDZ | TZ | aTZ | QZ | aQZ | FD |
|-------------------------------|-------------------------------|-----------------------|-----------------------|-----------------------|-----------------------|-----------------------|-----------------------|-----------------------|
| H ₂ | $\langle \hat{p}_e^x \rangle$ | 7.94×10^{-4} | 1.41×10^{-3} | 1.41×10^{-3} | 1.42×10^{-3} | 1.43×10^{-3} | 1.43×10^{-3} | 1.43×10^{-3} |
| | $\langle \hat{p}_e^y \rangle$ | 0.00 | 7.69×10^{-4} | 1.41×10^{-3} | 1.20×10^{-3} | 1.43×10^{-3} | 1.33×10^{-3} | 1.43×10^{-3} |
| LiH | $\langle \hat{p}_e^x \rangle$ | 2.83×10^{-4} | 7.77×10^{-4} | 9.07×10^{-4} | 1.10×10^{-3} | 1.16×10^{-3} | 1.28×10^{-3} | 1.31×10^{-3} |
| | $\langle \hat{p}_e^y \rangle$ | 2.22×10^{-4} | 6.07×10^{-4} | 7.51×10^{-4} | 9.14×10^{-4} | 1.01×10^{-3} | 1.21×10^{-3} | 1.25×10^{-3} |
| HCN | $\langle \hat{p}_e^x \rangle$ | 1.18×10^{-3} | 2.09×10^{-3} | 2.16×10^{-3} | 2.39×10^{-3} | 2.43×10^{-3} | 2.62×10^{-3} | 2.63×10^{-3} |
| | $\langle \hat{p}_e^y \rangle$ | 1.80×10^{-4} | 1.63×10^{-3} | 2.00×10^{-3} | 2.25×10^{-3} | 2.38×10^{-3} | 2.57×10^{-3} | 2.61×10^{-3} |
| H ₂ O ^a | $\langle \hat{p}_e^x \rangle$ | 5.06×10^{-4} | 1.63×10^{-3} | 1.93×10^{-3} | 2.09×10^{-3} | 2.18×10^{-3} | 2.28×10^{-3} | 2.32×10^{-3} |
| | $\langle \hat{p}_e^y \rangle$ | 4.47×10^{-4} | 1.60×10^{-3} | 1.92×10^{-3} | 2.08×10^{-3} | 2.18×10^{-3} | 2.28×10^{-3} | 2.32×10^{-3} |
| | $\langle \hat{p}_e^z \rangle$ | 2.03×10^{-5} | 1.39×10^{-3} | 1.86×10^{-3} | 2.01×10^{-3} | 2.16×10^{-3} | 2.24×10^{-3} | 2.31×10^{-3} |

^aFor the triatomic water molecule, we report the electronic momentum in the x -direction—assuming we translate the molecule in the x -direction (so forth for the y and z directions). For the FD approach, assuming we translate along the x -direction, we find $\langle \hat{p}_e^y \rangle = \langle \hat{p}_e^z \rangle = 0$ and so all relevant information is included in Table I. For the phase-space approach, $\langle \hat{p}_e^y \rangle$ can be non-zero, but the momentum is usually at least two orders of magnitude smaller than $\langle \hat{p}_e^x \rangle$, and so is not included in the table either.

Proceeding as we did above between Eqs. (54) and (60), it follows that

$$\langle \Psi_I | \hat{L}_e | \Psi_I \rangle = m_e \frac{d}{dt} \langle \Phi_I | r_e^2 \hat{\theta} | \Phi_I \rangle = m_e r_e^2 \frac{d}{dt} \int \theta |\Phi_I(\theta)|^2 d\theta. \quad (63)$$

For a linear or nearly linear molecule aligned along the x axis, let us make the assumption that the electronic density is localized around $\theta = 0$ and $\theta = \pi$ (but vanishes around $\theta = \pm\pi/2$). In such a case, we can expand the Cartesian coordinates $(x, y) = (r_e \cos(\theta), r_e \sin(\theta))$ around $\theta = 0$ and $\theta = \pi$ and obtain $(x, y)|_{\theta=0} \approx (r_e, r_e\theta)$ and $(x, y)|_{\theta=\pi} \approx (-r_e, -r_e(\theta-\pi))$ at the zeroth order, respectively. Therefore, in the vicinity of $\theta = 0$, $xy = r_e^2 \theta$; in the vicinity of $\theta = \pi$, $xy = r_e^2 \theta - r_e^2 \pi$. Note that because the integral $\langle \Phi_I | -\pi r_e^2 | \Phi_I \rangle$ is a constant (for a rigid rotor with r_e fixed), this term gives zero when taking the time derivative. Therefore, we can evaluate the final integral as

$$m_e \frac{d}{dt} \langle \Phi_I | r_e^2 \hat{\theta} | \Phi_I \rangle = m_e \frac{d}{dt} \langle \Phi_I | \hat{x} \hat{y} | \Phi_I \rangle = -\frac{d}{dt} \mathcal{I}_{xy}. \quad (64)$$

Below, we will check whether our electronic phase-space Hamiltonian satisfies Eq. (64) for the case of linear molecules undergoing rigid rotation.

IV. NUMERICAL RESULTS

We will now present numerical results testing the ability of our proposed phase-space electronic Hamiltonian in Eq. (9) to recover the correct linear and angular momentum. Our numerical results are within a Hartree–Fock (HF) framework that, though not exact, should offer a good enough starting point. The benchmarks for linear and angular momentum were computed by a finite-difference (FD) Hartree–Fock approach according to Eqs. (60) and (64), respectively. All the geometries used were optimized at the HF level with a cc-pVTZ basis set, and the coordinates are given in Appendix B. We investigate the effects of different basis sets, and

TABLE II. The nonzero components of the linear momentum (\hbar/a_0) calculated with a velocity that corresponds to stretching one H atom along the x axis. All the linear molecules are aligned along the x axis. The finite-difference (FD) approach serves as the benchmark and the results converge with larger basis sets. The linear momentum calculated with the phase-space Hamiltonian matches qualitatively the finite-difference values for reasonably large basis sets.

| | | STO-3G | DZ | aDZ | TZ | aTZ | QZ | aQZ |
|----------|-------------------------------|------------------------|------------------------|------------------------|------------------------|------------------------|------------------------|------------------------|
| H_2 | $\langle \hat{p}_e^x \rangle$ | 5.62×10^{-4} | 9.96×10^{-4} | 9.99×10^{-4} | 1.00×10^{-3} | 1.01×10^{-3} | 1.01×10^{-3} | 1.01×10^{-3} |
| | FD | 1.01×10^{-3} |
| LiH | $\langle \hat{p}_e^x \rangle$ | 1.87×10^{-4} | 7.17×10^{-4} | 9.62×10^{-4} | 5.68×10^{-4} | 4.26×10^{-4} | 4.48×10^{-4} | 2.01×10^{-4} |
| | FD | 1.07×10^{-3} | 1.45×10^{-3} | 1.48×10^{-3} | 1.50×10^{-3} | 1.51×10^{-3} | 1.50×10^{-3} | 1.51×10^{-3} |
| HCN | $\langle \hat{p}_e^x \rangle$ | 5.30×10^{-4} | 6.76×10^{-4} | 9.54×10^{-4} | 1.02×10^{-3} | 7.09×10^{-4} | 1.14×10^{-3} | 7.34×10^{-4} |
| | FD | 6.16×10^{-4} | 7.16×10^{-4} | 7.24×10^{-4} | 7.34×10^{-4} | 7.25×10^{-4} | 7.27×10^{-4} | 7.26×10^{-4} |
| H_2O^a | $\langle \hat{p}_e^x \rangle$ | 3.57×10^{-4} | 7.11×10^{-4} | 6.67×10^{-4} | 2.75×10^{-4} | 5.13×10^{-4} | 2.03×10^{-4} | 7.74×10^{-4} |
| | FD | 1.17×10^{-3} | 8.16×10^{-4} | 8.06×10^{-4} | 8.19×10^{-4} | 8.02×10^{-4} | 8.09×10^{-4} | 8.02×10^{-4} |
| | $\langle \hat{p}_e^y \rangle$ | 5.82×10^{-6} | -6.86×10^{-5} | -4.20×10^{-5} | -1.08×10^{-4} | -1.21×10^{-5} | -1.96×10^{-4} | -7.21×10^{-5} |
| | FD | -4.59×10^{-5} | -1.96×10^{-5} | -5.07×10^{-5} | -3.98×10^{-5} | -5.01×10^{-5} | -4.57×10^{-5} | -5.05×10^{-5} |

^aThe water molecule is placed in the xy plane with one of the O–H bonds aligned along the x-axis. Stretching this O–H bond along the x axis yields a relatively large linear momentum in the x direction ($\langle \hat{p}_e^x \rangle$) and a relatively small linear momentum in the y direction ($\langle \hat{p}_e^y \rangle$).

TABLE III. The z components of the angular momentum (\hbar) calculated with a velocity that corresponds to a rigid rotation around the z axis. All the linear molecules were aligned along the x axis with the center of mass placed at the origin. The finite-difference (FD) approach serves as the benchmark and converges quickly with larger basis sets. The angular momentum calculated with the phase-space Hamiltonian agrees reasonably well with the finite-difference values given a decent size of basis sets. The agreement improves at the stretched geometry of H_2 as the majority of the density distribution resides within a small angle with respect to the x axis.

| | | STO-3G | DZ | aDZ | TZ | aTZ | QZ | aQZ |
|-----------------|-------------------------------|-----------------------|-----------------------|-----------------------|-----------------------|-----------------------|-----------------------|-----------------------|
| H_2 | $\langle \hat{L}_e^z \rangle$ | 0.00 | 5.28×10^{-5} | 7.50×10^{-5} | 7.21×10^{-5} | 7.28×10^{-5} | 7.29×10^{-5} | 7.35×10^{-5} |
| | FD | 5.71×10^{-4} | 4.58×10^{-4} | 4.53×10^{-4} | 4.42×10^{-4} | 4.11×10^{-4} | 4.25×10^{-4} | 4.15×10^{-4} |
| Stretched H_2 | $\langle \hat{L}_e^z \rangle$ | 0.00 | 6.91×10^{-3} | 2.26×10^{-2} | 1.34×10^{-2} | 2.36×10^{-2} | 1.70×10^{-2} | 2.38×10^{-2} |
| | FD | 4.84×10^{-3} | 2.76×10^{-2} | 2.61×10^{-2} | 2.72×10^{-2} | 2.60×10^{-2} | 2.69×10^{-2} | 2.59×10^{-2} |
| LiH | $\langle \hat{L}_e^z \rangle$ | 5.74×10^{-3} | 9.38×10^{-3} | 1.07×10^{-2} | 1.07×10^{-2} | 1.12×10^{-2} | 1.11×10^{-2} | 1.13×10^{-2} |
| | FD | 7.57×10^{-3} | 8.98×10^{-3} | 9.27×10^{-3} | 9.37×10^{-3} | 9.50×10^{-3} | 9.46×10^{-3} | 9.51×10^{-3} |
| HCN | $\langle \hat{L}_e^z \rangle$ | 2.47×10^{-3} | 3.49×10^{-3} | 3.70×10^{-3} | 3.98×10^{-3} | 4.05×10^{-3} | 4.25×10^{-3} | 4.27×10^{-3} |
| | FD | 3.80×10^{-3} | 3.62×10^{-3} | 3.60×10^{-3} | 3.60×10^{-3} | 3.59×10^{-3} | 3.60×10^{-3} | 3.59×10^{-3} |
| C_2H_2 | $\langle \hat{L}_e^z \rangle$ | 1.54×10^{-3} | 7.49×10^{-3} | 8.88×10^{-3} | 9.71×10^{-3} | 1.03×10^{-2} | 1.09×10^{-2} | 1.11×10^{-2} |
| | FD | 1.14×10^{-2} | 1.13×10^{-2} |

use the acronyms XZ for cc-pVXZ and aXZ for aug-cc-pVXZ basis sets in Tables I–VI. All the linear molecules are aligned along the x axis.

We begin by checking the accuracy of the linear electronic momentum as computed with the phase-space Hamiltonian when the entire molecule translates. In Table I, we show the α components of the linear momentum as calculated with a translation velocity along the α axis and a magnitude corresponding to room temperature thermal motion. The FD approach uses a time step of 1 a.u. (1 a.u. = 0.0242 fs). The linear momentum values calculated with the FD approach [Eq. (60)] serve as the benchmark and do not change much at all with different basis sets for translation motion. According to Table I, the linear momentum calculated with the

phase-space Hamiltonian approaches does converge to the finite-difference values for larger basis sets. This convergence demonstrates that, despite using a single state, the practical phase-space method at the Hartree–Fock level can effectively capture the electronic motion going slightly beyond the BO approximation—when given a reasonably large basis set. Note that adding the one-electron rotation factor Γ'' does not change the results in Table I at all due to the invariance of Γ'' with respect to translation, $\sum_A \Gamma''_{\mu\nu}^{A\alpha} = 0$.

Next, we examine the linear momentum for internal motion. In Table II, we report the linear momentum when moving only the H atom with a velocity that again corresponds to room temperature thermal motion. According to Table II, the linear momentum calculated with the FD approach does converge with larger basis sets.

TABLE IV. $\langle \hat{L}_e^z \rangle$ values (\hbar) as calculated for a rigid rotation of one LiH molecule in the absence and in the presence of another molecule located far away in space. Because of the large distance between the molecules, the angular momentum of the first LiH molecule should be the same in both calculations. The phase-space approach results are reported with $\Gamma = \Gamma'$ only and $\Gamma = \Gamma' + \Gamma''$. When Γ'' is included, two choices of the locality parameter $w = 0$ (non-local) and $w = 0.3$ (semi-local) are investigated for the two LiH systems. (For the single LiH system, $w = 0$ and $w = 0.3$ give the same results.) Only the $w = 0.3$ data give consistent results for the LiH molecule. The data here prove conclusively that one cannot pick $w = 0$ (and ignore locality) if one seeks meaningful results.

| | | STO-3G | DZ | aDZ | TZ | aTZ | QZ | aQZ |
|------------|-------------------------------|-----------------------|-----------------------|-----------------------|-----------------------|-----------------------|-----------------------|-----------------------|
| Two LiH | Γ' | 9.11×10^{-4} | 3.50×10^{-3} | 6.22×10^{-3} | 4.93×10^{-3} | 7.55×10^{-3} | 5.77×10^{-3} | 6.85×10^{-3} |
| | $\Gamma' + \Gamma''(w = 0)$ | 6.27×10^{-4} | 3.15×10^{-3} | 5.96×10^{-3} | 4.59×10^{-3} | 7.33×10^{-3} | 5.46×10^{-3} | 6.58×10^{-3} |
| | $\Gamma' + \Gamma''(w = 0.3)$ | 5.74×10^{-3} | 9.38×10^{-3} | 1.07×10^{-2} | 1.07×10^{-2} | 1.12×10^{-2} | 1.11×10^{-2} | 1.13×10^{-2} |
| Single LiH | Γ' | 9.11×10^{-4} | 3.50×10^{-3} | 6.22×10^{-3} | 4.93×10^{-3} | 7.55×10^{-3} | 5.77×10^{-3} | 6.85×10^{-3} |
| | $\Gamma' + \Gamma''$ | 5.74×10^{-3} | 9.38×10^{-3} | 1.07×10^{-2} | 1.07×10^{-2} | 1.12×10^{-2} | 1.11×10^{-2} | 1.13×10^{-2} |
| | FD | 7.57×10^{-3} | 8.98×10^{-3} | 9.27×10^{-3} | 9.37×10^{-3} | 9.50×10^{-3} | 9.46×10^{-3} | 9.51×10^{-3} |

By contrast, for molecules other than the H₂ molecule, the linear momentum as calculated with our phase-space approach does not converge as well with larger basis sets, insofar as diffuse functions clearly create differences. Nevertheless, when a decently sized non-augmented basis set is used, such as a cc-pVDZ basis set, we find that the linear momenta calculated with the two approaches does agree at least qualitatively. Note that, here, the one-electron rotational factor Γ'' has not been included. Including the rotational factor changes the results of the H₂O molecule by only a small amount, as given in Table V in Appendix C.

The discrepancies between the two approaches in Table II can be understood as follows for the specific case of an HF ansatz. Let us write out Nafie's expression for the electronic momentum in an AO basis (where $D_{\nu\mu}$ is the relevant density matrix),

$$\langle \hat{\mathbf{p}}_e \rangle = m_e \frac{d}{dt} \langle \hat{\mathbf{r}}_e \rangle \quad (65)$$

$$= m_e \frac{d}{dt} \sum_{\mu\nu} D_{\nu\mu} \mathbf{r}_{\mu\nu} \quad (66)$$

$$= m_e \sum_{\mu\nu} \left(\frac{d}{dt} D_{\nu\mu} \cdot \mathbf{r}_{\mu\nu} + D_{\nu\mu} \cdot \frac{d}{dt} \mathbf{r}_{\mu\nu} \right). \quad (67)$$

The first term accounts for the fact that the density matrix (in a moving AO basis) changes as a function of time (the so-called orbital response); the second term accounts for the fact that the AO basis itself changes as a function of time. For the ideal case of an H-atom with the electron in a 1s orbital, the first term would be zero while the second term would be nonzero. In view of this analysis, it is clear that our proposed phase-space electronic Hamiltonian captures all of the physics in the second term but not the physics in the first term (to the lowest order). In practice, whenever the systems pass through a crossing with another state, the $\frac{d}{dt} D_{\nu\mu}$ term will get larger, and we will not capture such nonadiabatic effects.

In order to further probe how much of the electronic momentum depends on nonadiabaticity, we have investigated the electronic momentum as a function of bond distance for the case of LiH molecule, a molecule where curve crossings are known to occur at large separation. In Fig. 1, we plot the linear momentum calculated with the phase-space restricted HF (blue solid line) and unrestricted HF (red dashed line) approaches and with the FD approach with restricted HF (gray solid line) and unrestricted HF (purple dotted line).

line). The equilibrium bond distance is 3.0374 bohrs, and we set the hydrogen momentum to be $P_H = 1.8$ a.u. (i.e., $v_H = 0.001$ a.u.); here, a positive value of P_H stretches the molecule. Between 2 and 8 bohrs, there is a Coulson–Fischer (CF) point at ~4.3 bohrs, where the HF state transitions from closed shell (ionic) to open shell (biradical). Around this CF point, the FD unrestricted approach yields a negative spike in linear momentum. Physically, when we increase the bond distance, there is a large decrease in the electronic position expectation value $\langle \Phi_I | \hat{x} | \Phi_I \rangle$ because, as the molecule transitions from the ionic configuration (Li^{δ+}–H^{δ-}) to a biradical configuration (Li^{*}–H^{*}), and electron jumps back from the H nucleus to the Li nucleus. At this CF point, where the orbital response is enormous, obviously, the two expressions for electron linear momentum

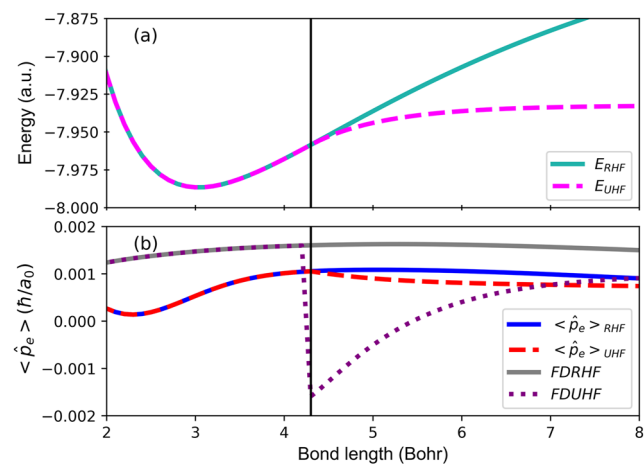


FIG. 1. (a) RHF and UHF potential energy surfaces drawn with a cyan solid line and a magenta dashed line, respectively. (b) The linear momentum calculated with the phase-space restricted HF (blue solid line), phase-space unrestricted HF (red dashed line), the FD restricted HF (gray solid line), and FD unrestricted (purple dotted line). The equilibrium bond distance is 3.0374 bohrs. The location of the Coulson–Fischer point is shown by the black solid line, where the internal nuclear motion changes the electronic wavefunction discontinuously so that the FD approach predicts a spike in the linear momentum. The phase-space HF approach does not take into account the orbital response to the nuclear motion and yields a smoother prediction in this region. In this figure, we have set $P_H = 1.8$ a.u. (i.e., $v_H = 0.001$ a.u.).

(phase-space vs finite difference) strongly disagree—but otherwise, they are in the same order of magnitude.

Next, let us compare the angular momentum calculated with the phase-space approach and the finite difference approach according to Eq. (64). In Table III, we show the angular momentum computed with both approaches for molecules at both the equilibrium and stretched geometries. The bond lengths for the stretched geometry were 8 bohrs. All of the molecules are placed with their center of mass at the origin and are aligned along the x -axis. A velocity corresponding to a rigid rotation around the z -axis was applied. For the diatomic molecules, this velocity corresponded to a rotation of the whole molecule by 0.05° per time step (1 a.u.). For the polyatomic molecules, a smaller velocity was chosen such that the total rotational kinetic energy corresponded to room-temperature thermal motion; as above, for the FD calculations, we set the time step to be 1 a.u. For the equilibrium geometries, we find the angular momentum calculated with the phase-space and the finite-difference approaches are about the same magnitude for reasonably sized basis sets. This agreement improves for the stretched geometry, which makes sense given the assumptions in Eq. (64). After all, we assumed there that the angle of the electronic density in the xy plane was centered mostly around $\theta = 0$ and $\theta = \pi$ and if we compare stretched vs equilibrium geometries, we find that the electronic density centered around the origin is much less in the former (rather than later) geometries. The results of the phase-space approach in Table III use $\Gamma = \Gamma' + \Gamma''$. In Table VI in Appendix C, we further show that the contribution of Γ'' can be about the same or one magnitude smaller than the contribution of Γ' .

V. DISCUSSION: SEMI-LOCALITY OF Γ''

As discussed above [as well as in Ref. 30 and the companion paper (Ref. 25)], the ERF term Γ'' cannot be made strictly local—unlike the ETF term Γ' . To that end, in Eq. (47), we introduced a parameter w to control the locality of Γ'' . Now, the results in Tables II and III are not very sensitive to the choice of parameter w . One might wonder: does this insensitively imply that w is not of practical importance? Or is the insensitivity perhaps just a consequence of the fact that we modeled small molecules exclusively in the tables above. To prove that the former is false and the latter is correct, i.e., that semi-locality of Γ'' is indeed crucial for a physically meaningful effect, in this section, we will work with simple numerical examples illustrating how and why maintaining size consistency is essential.

Let us consider one rigidly rotating LiH molecule (studied in Table III) at the origin and add a second LiH molecule around ~35 bohrs away (see Appendix B for the geometry of this LiH dimer). One expects that the second LiH molecule, located far away, should not affect the angular momentum resulting from the rigid rotation of the original LiH molecule. In Table IV, we list $\langle \hat{L}_e^z \rangle$ values for the original LiH molecule as calculated either when the molecule is isolated (same data as from Tables III and VI) or in the presence of second LiH molecule. We present data from both $w = 0$ (corresponding to no locality) and $w = 0.3$ (corresponding to semi-locality) calculations. Note that the results calculated with semi-locality ($w = 0.3$) match with the $\langle \hat{L}_e^z \rangle$ calculated for the single LiH system, indicating that the second LiH molecule far away correctly has negligible impact on the $\langle \hat{L}_e^z \rangle$ values. By contrast,

without any locality constraint ($w = 0$), the $\langle \hat{L}_e^z \rangle$ values are different (incorrectly).

As a side note, in Table IV, we also list the $\langle \hat{L}_e^z \rangle$ values as calculated with only the ETF term $\Gamma = \Gamma'$. Here, the single and double LiH systems yield the same exact expectation values as one should expect from size consistency—again because Γ' is strictly local. That being said, in Table IV, we find that the results with $w = 0$ for the double LiH case are very similar to those with Γ' alone; clearly, the Γ'' contribution to $\langle \hat{L}_e^z \rangle$ values becomes too small if one does not enforce locality on the ERF matrix elements.

VI. DISCUSSION: IMPLICATIONS FOR NONADIABATIC DYNAMICS

The theory and results above present a reasonably compelling argument that, in the future, one can improve upon Born–Oppenheimer dynamics simply by working with a phase-space electronic Hamiltonian that depends on both nuclear position and momentum. Admittedly, the data gathered here are still limited. We have checked for the electronic linear momentum with regard to internal motion, but we have not yet checked for the electronic angular momentum with regard to internal motion (only with regard to rigid motion). Checking for internal motion will require a large basis and an exact full configuration interaction (FCI) calculation in order to evaluate the exact angular momentum through the exact sum over states expansion in Eq. (53). Such a daunting task will probably be necessary in the future. Nevertheless, notwithstanding its limited nature, the data gathered so far are quite encouraging and have the potential to open up new areas of study.⁶⁹

Obviously, launching dynamical simulations in the near future will be the next logical step. To that end, note first that the Γ -couplings are one-electron operators such that diagonalizing the resulting phase-space electronic Hamiltonian should require a trivial added cost. The same cost analysis holds for the gradients of this phase-space electronic Hamiltonian, such that running *ab initio* dynamics should be readily possible. Moreover, one can imagine running both single surface dynamics (analogous to BO dynamics) as well as nonadiabatic surface hopping dynamics. In the spirit of Ref. 16, we can be confident that all such dynamics will both predict nonzero electronic angular momentum while also conserving the total angular momentum. To date, the only semiclassical nonadiabatic algorithm for simulating such dynamics has been through the exact factorization approach⁷⁰ (which is another promising approach but still under development).^{71–73}

Another obvious target of the current research is the calculation of vibrational circular dichroism (VCD) spectra.^{74–77} Indeed, the inability of standard BO theory to calculate VCD spectra stimulated the original work of Nafie,^{19,20,78,79} and now many others,^{80–86} to go beyond BO theory and construct the relevant matrix elements (with electronic angular momentum along the ground state) that allowed for a nonzero vibrational rotatory strength. While the present phase-space approach has many similarities with the nuclear velocity perturbation (NVP) approach in Refs. 20 and 87–89, it is worth noting that with a phase-space electronic Hamiltonian, apparently, one can calculate a nonzero rotatory strength without doing a double response theory (albeit at the cost of ignoring orbital response). Thus, the present approach would appear to be a natural starting point for VCD calculations in the future.⁹⁰

Although not addressed above, it is crucial to emphasize that all of the theories above are generalized to include spin degrees of freedom. In such a case, as discussed in the Conclusion and Outlook section in Ref. 25, one needs only modify the form of Γ'' to include spin degrees of freedom, and the total angular momentum is conserved (without explicitly including a Berry force). In recent years, there has been an explosion of interest in coupled nuclear-electronic-spin motion, highlighted by the possibility that nuclear motion (and chiral phonons) may yield new insight into the chiral-induced spin selectivity (CISS) effect,^{91–95} whereby electronic motion through molecular systems shows clear signs of spin preference. Beyond CISS, one can also imagine running similar dynamics to explore spin polarization in intersystem crossing more generally.^{96–100}

Finally, beyond dynamics, one can envision that because the chemistry and physics communities are less experienced with phase-space Hamiltonians than with standard electronic Hamiltonians, new tools will be needed in the future. From a bird's eye view, as far as the electrons are concerned, a phase-space electronic Hamiltonian breaks time-reversal symmetry and is equivalent to introducing a fluctuating magnetic field, and thus, advanced statistical mechanics sampling methods will be needed. If there are spin degrees of freedom, these statistical mechanics methods will need to be compatible with closely spaced, nearly, or fully degenerate electronic states. Finally, the problems will be only richer if we include explicit magnetic fields^{101–103} as well.

At the end of the day, once the computational tools have been built, there is the potential to use the current phase-space approach so as to generalize the well-known Marcus parabolas^{104,105} to include spin degrees of freedom and to study how spin affects electron transfer and curve crossings in a manner which conserves angular momentum. This approach should allow us to explore very new physics involving the flow of angular momentum between nuclear, electronic, and spin degrees of freedom.

VII. SUMMARY

In this paper, we have proposed a phase-space electronic Hamiltonian $H_{PS}(X, P)$ with an effective one-electron operator $\Gamma_{\mu\nu}$ that couples electronic motion to the nuclear momentum P . Our ansatz is that one can build the Γ -couplings using previously derived electron-translation and electron-rotation factors. These matrix elements satisfy Eqs. (18)–(21') so that, by including the $\Gamma \cdot P$ term, one naturally conserves the total linear and angular momentum, allowing the electronic and nuclear degrees of freedom to exchange linear and angular momentum. Moreover, our initial data suggest that, for this choice of Γ , one can qualitatively recover the correct electronic linear momentum in agreement with Nafie's theory, as well as the correct electronic angular momentum (albeit for the case of rigid motion), which represent important post-Born–Oppenheimer benchmarks.

Looking forward, because $\Gamma_{\mu\nu}$ is a one-electron operator, diagonalizing $H_{PS}(X, P)$ requires the same computational cost as solving a standard electronic Hamiltonian $H_{el}(X)$ as far as the electronic structure is concerned. Thus, the phase-space electronic approach proposed here offers a physically meaningful as well as computationally practical framework for recovering coupled nonadiabatic nuclear-electronic-spin dynamics, going beyond

electrostatic studies of non-Born–Oppenheimer dynamic and establishing a crucial link between the chemical dynamics and spintronic problems.

ACKNOWLEDGMENTS

The authors thanked Al Viggiano, Nick Schuman, and Shaun Ard for focusing their attention on the problem of angular momentum conservation and thanked Clàudia Climent and Vishikha Athavale for helpful conversations in developing the relevant matrix elements and equations of motion. This work was supported by the National Science Foundation (Grant No. CHE-2102402).

AUTHOR DECLARATIONS

Conflict of Interest

The authors have no conflicts to disclose.

Author Contributions

Zhen Tao: Data curation (lead); Investigation (equal); Software (equal); Writing – original draft (equal). **Tian Qiu:** Data curation (supporting); Investigation (equal); Writing – review & editing (supporting). **Mansi Bhati:** Data curation (supporting); Software (equal). **Xuezhi Bian:** Conceptualization (supporting); Data curation (supporting); Investigation (supporting); Writing – review & editing (supporting). **Titouan Duston:** Investigation (supporting); Writing – review & editing (supporting). **Jonathan Rawlinson:** Conceptualization (supporting); Writing – review & editing (supporting). **Robert G. Littlejohn:** Conceptualization (supporting); Writing – review & editing (supporting). **Joseph E. Subotnik:** Conceptualization (lead); Investigation (equal); Methodology (lead); Writing – original draft (equal).

DATA AVAILABILITY

The data that supports the findings of this study are available within the article.

APPENDIX A: ROTATIONS OF ATOMIC ORBITAL MATRIX ELEMENTS

1. Overview

In this appendix, we will derive the fundamental (intuitive) rules that govern how the one and two electron operators transform under rotation, as well as how the linear and angular momentum transform. Let R be a rotational operator in Cartesian xyz space that rotates around the axis $\delta/|\delta|$ by an amount $|\delta|$: $R = \exp(-\frac{i}{\hbar} \sum_{\alpha} L^{\alpha} \delta_{\alpha})$. Let $|v_B\rangle$ be a basis function on atomic center B and let $|\tilde{v}_B\rangle$ be a rotation of that basis function around center B, $|\tilde{v}_B\rangle = \exp(-\frac{i}{\hbar} \sum_{\alpha} \hat{L}_e^{B\alpha} \delta_{\alpha}) |v_B\rangle$, where

$$\hat{L}_e^{B\alpha} = -i\hbar \sum_{\beta\gamma} \epsilon_{\alpha\beta\gamma} (r_{\beta} - X_{B\beta}) \frac{\partial}{\partial r^{\gamma}} = \hat{L}_e^{\alpha} - \sum_{\beta\gamma} \epsilon_{\alpha\beta\gamma} X_{B\beta} \hat{p}_e^{\gamma}. \quad (\text{A1})$$

We will prove

$$h_{\bar{\mu}\bar{\nu}}(\mathbf{R}X_0) = h_{\mu\nu}(X_0), \quad (\text{A2})$$

$$P_{\bar{\mu}\bar{\nu}}(\mathbf{R}X_0) = R P_{\mu\nu}(X_0), \quad (\text{A3})$$

$$J_{\bar{\mu}\bar{\nu}}(\mathbf{R}X_0) = R J_{\mu\nu}(X_0), \quad (\text{A4})$$

$$\pi_{\bar{\mu}\bar{\nu}\bar{\lambda}\bar{\sigma}}(\mathbf{R}X_0) = \pi_{\mu\nu\lambda\sigma}(X_0). \quad (\text{A5})$$

These relationships are broadly important both for the results in this manuscript as well as those in Ref. 25. We will also prove below the equivalence of Eqs. (21) and (21').

2. Overview of one-electron operator atomic orbital matrix elements

Let us write the matrix elements for general one-electron operator \hat{O}^1 in atom-centered basis as $\mathcal{O}_{\mu_A v_B}^1(X_0)$, where the basis function μ is centered on atom A and v is centered on atom B. We imagine performing two rotations: (i) first, we rotate the whole molecule $\mathbf{R}X_0$ and (ii) second, we rotate the basis functions around their atomic centers. We wish to evaluate the first-order change of the matrix element of the general one-electron operator $\mathcal{O}_{\bar{\mu}_A \bar{v}_B}^1(\mathbf{R}X_0)$,

$$\zeta(\delta) = \mathcal{O}_{\bar{\mu}_A \bar{v}_B}^1(\mathbf{R}X_0) - \mathcal{O}_{\mu_A v_B}^1(X_0) - O(\delta^2). \quad (\text{A6})$$

We will compute the contributions of the two rotations above to $\zeta(\delta)$ separately.

1. If we ignore the change in orbitals, the first order change in the matrix elements due to the molecular rotation $R \approx 1 - \frac{i}{\hbar} \sum_{\alpha} L^{\alpha} \delta_{\alpha}$ is

$$\begin{aligned} \mathcal{O}_{\mu_A v_B}^1(\mathbf{R}X_0) - \mathcal{O}_{\mu_A v_B}^1(X_0) &\approx \frac{-i}{\hbar} \sum_{C\alpha\beta\gamma} \delta_{\alpha} \frac{\partial \mathcal{O}_{\mu_A v_B}^1}{\partial X_{C\gamma}} (L_{\gamma\beta}^{\alpha} X_{C\beta}) \\ &= \sum_{C\alpha\beta\gamma} \delta_{\alpha} \epsilon_{\beta\gamma\alpha} X_{C\beta} \frac{\partial \mathcal{O}_{\mu_A v_B}^1}{\partial X_{C\gamma}}. \end{aligned} \quad (\text{A7})$$

Here, we have used the relationship $L_{\beta\gamma}^{\alpha} = -i\hbar\epsilon_{\alpha\beta\gamma}$. We can further expand the nuclear derivatives of the one-electron matrix elements into three components,

$$\begin{aligned} \frac{\partial \mathcal{O}_{\mu_A v_B}^1}{\partial X_{C\gamma}} &= \left\langle \mu_A \left| \frac{\partial \hat{O}^1}{\partial X_{C\gamma}} \right| v_B \right\rangle \\ &+ \left\langle \frac{\partial}{\partial X_{Ay}} \mu_A \left| \hat{O}^1 \right| v_B \right\rangle \delta_{AC} + \left\langle \mu_A \left| \hat{O}^1 \right| \frac{\partial}{\partial X_{By}} v_B \right\rangle \delta_{BC}. \end{aligned} \quad (\text{A8})$$

2. Next, we compute the first-order change due to rotating the atomic basis functions around their centers. Considering the first order change in δ_{α} for $|v_B\rangle$ for example, we find

$$|\bar{v}_B\rangle \approx \left(1 - \frac{i}{\hbar} \sum_{\alpha} \hat{L}_e^{B\alpha} \delta_{\alpha} \right) |v_B\rangle. \quad (\text{A9})$$

If we plug in Eq. (A1), we can evaluate the contribution to the first-order change,

$$\begin{aligned} \mathcal{O}_{\bar{\mu}_A \bar{v}_B}^1(\mathbf{R}X_0) - \mathcal{O}_{\mu_A v_B}^1(\mathbf{R}X_0) \\ \approx \frac{-i}{\hbar} \sum_{\alpha} \delta_{\alpha} \left(\langle \mu_A | [\hat{O}^1, \hat{L}_e^{\alpha}] | v_B \rangle - \sum_{\beta\gamma} \epsilon_{\alpha\beta\gamma} X_{B\beta} \langle \mu_A | \hat{O}^1 | \hat{p}_e^{\gamma} v_B \rangle \right). \end{aligned} \quad (\text{A10})$$

Now, if we also add in the first order change in δ_{α} for $|\bar{\mu}_A\rangle$, we recover

$$\mathcal{O}_{\bar{\mu}_A \bar{v}_B}^1(\mathbf{R}X_0) - \mathcal{O}_{\mu_A v_B}^1(\mathbf{R}X_0) \quad (\text{A11})$$

$$\begin{aligned} \approx \frac{-i}{\hbar} \sum_{\alpha} \delta_{\alpha} \left[\langle \mu_A | [\hat{O}^1, \hat{L}_e^{\alpha}] | v_B \rangle + \sum_{\beta\gamma} \epsilon_{\alpha\beta\gamma} (X_{A\beta} \langle \hat{p}_e^{\gamma} \mu_A | \hat{O}^1 | v_B \rangle \right. \\ \left. - X_{B\beta} \langle \mu_A | \hat{O}^1 | \hat{p}_e^{\gamma} v_B \rangle) \right]. \end{aligned}$$

Finally, if we use the relationship $(\hat{p}_e^{\gamma} - i\hbar\nabla_n^{\gamma})|v_B\rangle = 0$, the second term in Eq. (A11) becomes

$$\begin{aligned} \frac{-i}{\hbar} \sum_{\alpha\beta\gamma} \delta_{\alpha} \epsilon_{\alpha\beta\gamma} (X_{A\beta} \langle \hat{p}_e^{\gamma} \mu_A | \hat{O}^1 | v_B \rangle - X_{B\beta} \langle \mu_A | \hat{O}^1 | \hat{p}_e^{\gamma} v_B \rangle) \\ = - \sum_{\alpha\beta\gamma} \delta_{\alpha} \epsilon_{\alpha\beta\gamma} \left(X_{A\beta} \left\langle \frac{\partial \mu_A}{\partial X_{Ay}} \right| \hat{O}^1 | v_B \rangle + X_{B\beta} \langle \mu_A | \hat{O}^1 \left| \frac{\partial v_B}{\partial X_{By}} \right. \right). \end{aligned} \quad (\text{A12})$$

Finally, adding these two contributions together and noting that the last two terms in Eq. (A8) cancel with the terms in Eq. (A12), we find

$$\zeta(\delta) = \sum_{C\alpha\beta\gamma} \delta_{\alpha} \epsilon_{\alpha\beta\gamma} X_{C\beta} \langle \mu_A | \frac{\partial \hat{O}^1}{\partial X_{C\gamma}} | v_B \rangle - \frac{i}{\hbar} \sum_{\alpha} \delta_{\alpha} \langle \mu_A | [\hat{O}^1, \hat{L}_e^{\alpha}] | v_B \rangle. \quad (\text{A13})$$

Equation (A13) is general and allows us to evaluate the first-order changes under rotation for different one-electron matrix elements.

a. One-electron core Hamiltonian matrix elements [proving Eq. (A2)]

Due to the isotropy of the space, the following commutator is zero:

$$[\hat{h}, \hat{L}_e^{\alpha} + \hat{L}_n^{\alpha}] = 0. \quad (\text{A14})$$

Plugging this commutation relation into Eq. (A13), the second term on the RHS becomes

$$\begin{aligned} \frac{-i}{\hbar} \sum_{\alpha} \delta_{\alpha} \langle \mu_A | [\hat{h}, \hat{L}_e^{\alpha}] | v_B \rangle &= \frac{i}{\hbar} \sum_{\alpha} \delta_{\alpha} \langle \mu_A | [\hat{h}, \hat{L}_n^{\alpha}] | v_B \rangle \\ &= - \sum_{C \alpha \beta \gamma} \delta_{\alpha} \epsilon_{\alpha \beta \gamma} X_{C \beta} \langle \mu_A | \frac{\partial \hat{h}}{\partial X_{C \gamma}} | v_B \rangle. \quad (\text{A15}) \end{aligned}$$

Plugging Eq. (A15) back to Eq. (A13), we see that two terms cancel with each other, thus proving Eq. (A2).

b. Electronic linear momentum matrix elements [proving Eq. (A3)]

We begin by evaluating the commutator,

$$[\hat{p}_e^{\eta}, \hat{L}_e^{\alpha}] = i\hbar \sum_{\gamma} \epsilon_{\eta \alpha \gamma} \hat{p}_e^{\gamma}. \quad (\text{A16})$$

Plugging this commutation relation in Eq. (A13), we find

$$\zeta(\delta) = \sum_{\alpha \gamma} \delta_{\alpha} \epsilon_{\eta \alpha \gamma} \langle \mu_A | \hat{p}_e^{\gamma} | v_B \rangle, \quad (\text{A17})$$

which is the first-order change corresponding to the RHS of Eq. (A3).

c. $J_{\mu_A v_B}$ matrix elements [proving Eq. (A4)]

We first review the definition of the $J_{\mu_A v_B}^{\eta}$ matrix elements,

$$J_{\mu_A v_B}^{\eta} = -\frac{i}{2\hbar} \langle \mu_A | (\hat{L}_e^{A\eta} + \hat{L}_e^{B\eta}) | v_B \rangle. \quad (\text{A18})$$

Now, we evaluate the commutation relation,

$$\begin{aligned} [\hat{L}_e^{A\eta}, \hat{L}_e^{\alpha}] &= \left[\hat{L}_e^{\eta} - \sum_{\beta \gamma} \epsilon_{\eta \beta \gamma} X_{A \beta} \hat{p}_e^{\gamma}, \hat{L}_e^{\alpha} \right] \\ &= i\hbar \sum_{\gamma} \epsilon_{\eta \alpha \gamma} \hat{L}_e^{\gamma} - i\hbar \sum_{\beta \gamma \kappa} \epsilon_{\eta \beta \gamma} X_{A \beta} \epsilon_{\gamma \alpha \kappa} \hat{p}_e^{\kappa}. \quad (\text{A19}) \end{aligned}$$

Plugging this commutation relation in Eq. (A13), we find

$$\begin{aligned} \zeta(\delta) &= \frac{i}{2\hbar} \sum_{\alpha \beta \gamma \kappa} \delta_{\alpha} \epsilon_{\alpha \beta \kappa} X_{A \beta} \epsilon_{\eta \kappa \gamma} \langle \mu_A | \hat{p}_e^{\gamma} | v_B \rangle - \frac{i}{2\hbar} \sum_{\alpha \gamma} \delta_{\alpha} \epsilon_{\eta \alpha \gamma} \\ &\times \langle \mu_A | \hat{L}_e^{\gamma} | v_B \rangle + \frac{i}{2\hbar} \sum_{\alpha \beta \gamma \kappa} \delta_{\alpha} \epsilon_{\eta \beta \gamma} X_{A \beta} \epsilon_{\gamma \alpha \kappa} \langle \mu_A | \hat{p}_e^{\kappa} | v_B \rangle. \quad (\text{A20}) \end{aligned}$$

This is the first order change for the term $-\frac{i}{2\hbar} \mathbf{R} \langle \mu_A | \hat{L}_e^A | v_B \rangle$. One can obtain the equivalent result for the $-\frac{i}{2\hbar} \mathbf{R} \langle \mu_A | \hat{L}_e^B | v_B \rangle$ term. Hence, we have proven Eq. (A4).

3. Two-electron operator atomic orbital matrix elements [proving Eq. (A5)]

The evaluation of the first-order changes in the two-electron operator matrix elements upon rotation is very similar to the approach above. Given a general two-electron operator $\hat{\mathcal{O}}^2$, the first order changes $\zeta(\delta)$ to the matrix elements upon rotation can be evaluated as follows:

- The first order change due to the molecular rotation $\mathbf{R} \approx 1 - \frac{i}{\hbar} \sum_{\alpha} \mathbf{L}^{\alpha} \delta_{\alpha}$ [similar to Eq. (A7)] is

$$\begin{aligned} \mathcal{O}_{\mu_A v_B \lambda_C \sigma_D}^2(\mathbf{R} \mathbf{X}_0) - \mathcal{O}_{\mu_A v_B \lambda_C \sigma_D}^2(\mathbf{X}_0) \\ \approx \frac{-i}{\hbar} \sum_{Q \alpha \beta \gamma} \delta_{\alpha} \frac{\partial \mathcal{O}_{\mu_A v_B \lambda_C \sigma_D}^2}{\partial X_{Q \gamma}}(L_{\gamma \beta}^{\alpha} X_{Q \beta}) \quad (\text{A21}) \end{aligned}$$

$$= \sum_{Q \alpha \beta \gamma} \delta_{\alpha} \epsilon_{\beta \gamma \alpha} X_{Q \beta} \frac{\partial \mathcal{O}_{\mu_A v_B \lambda_C \sigma_D}^2}{\partial X_{Q \gamma}}. \quad (\text{A22})$$

We can further expand the nuclear derivatives of the two-electron matrix elements into five components,

$$\begin{aligned} \frac{\partial \mathcal{O}_{\mu_A v_B \lambda_C \sigma_D}^2}{\partial X_{Q \gamma}} &= \langle \mu_A v_B | \frac{\partial \hat{\mathcal{O}}^2}{\partial X_{Q \gamma}} | \lambda_C \sigma_D \rangle + \left\langle \left(\frac{\partial}{\partial X_{A \gamma}} \mu_A \right) v_B \right| \\ &\times \hat{\mathcal{O}}^2 | \lambda_C \sigma_D \rangle \delta_{AG} + \left\langle \mu_A \frac{\partial}{\partial X_{B \gamma}} v_B \right| \hat{\mathcal{O}}^2 | \lambda_C \sigma_D \rangle \delta_{BG} \\ &+ \langle \mu_A v_B | \hat{\mathcal{O}}^2 \left| \left(\frac{\partial}{\partial X_{C \gamma}} \lambda_C \right) \sigma_D \right\rangle \delta_{CG} \\ &+ \langle \mu_A v_B | \hat{\mathcal{O}}^2 \left| \lambda_C \frac{\partial}{\partial X_{D \gamma}} \sigma_D \right\rangle \delta_{DG}. \quad (\text{A23}) \end{aligned}$$

- Similar to Eq. (A11), the first-order change due to the basis functions rotating around their centers can be written as

$$\begin{aligned} \mathcal{O}_{\tilde{\mu}_A \tilde{v}_B \tilde{\lambda}_C \tilde{\sigma}_D}^2 - \mathcal{O}_{\mu_A v_B \lambda_C \sigma_D}^2(\mathbf{X}_0) \\ \approx \frac{-i}{\hbar} \sum_{\alpha n} \delta_{\alpha} \langle \mu_A v_B | [\hat{\mathcal{O}}^2, \hat{L}_{e,n}^{\alpha}] | \lambda_C \sigma_D \rangle \\ - \frac{i}{\hbar} \sum_{\alpha \beta \gamma n} \delta_{\alpha} \epsilon_{\alpha \beta \gamma} [X_{A \beta} \langle \hat{p}_{e,n}^{\gamma} (\mu_A v_B) | \hat{\mathcal{O}}^2 | \lambda_C \sigma_D \rangle \\ - X_{B \beta} \langle \mu_A v_B | \hat{\mathcal{O}}^2 | \hat{p}_{e,n}^{\gamma} (\lambda_C \sigma_D) \rangle]. \quad (\text{A24}) \end{aligned}$$

Here, the letter n represents the electron number. For a two-electron operator, n can be either electron 1 or 2. When n refers to electron 1, \hat{L}_e^{α} acts on μ_A or λ_C . We note that the long second term on the RHS of Eq. (A24) cancels with the terms that involve nuclear derivatives of the basis functions in Eq. (A23). Hence, the first order change in the two-electron operator upon rotation is

$$\begin{aligned} \zeta(\delta) &= \sum_{Q \alpha \beta \gamma} \delta_{\alpha} \epsilon_{\beta \gamma \alpha} X_{Q \beta} \langle \mu_A v_B | \frac{\partial \hat{\mathcal{O}}^2}{\partial X_{Q \gamma}} | \lambda_C \sigma_D \rangle \\ &- \frac{i}{\hbar} \sum_{\alpha n} \delta_{\alpha} \langle \mu_A v_B | [\hat{\mathcal{O}}^2, \hat{L}_{e,n}^{\alpha}] | \lambda_C \sigma_D \rangle. \quad (\text{A25}) \end{aligned}$$

a. $\pi_{\mu_A v_B \lambda_C \sigma_D}$ matrix elements

From the form of the two-electron interaction operator $\frac{1}{|\mathbf{r}_1 - \mathbf{r}_2|}$, we can easily deduce that the first term in Eq. (A25) is zero. For the second term in Eq. (A25), note that

$$\left[\hat{\mathbf{r}}_1 \times \hat{\mathbf{p}}_1 + \hat{\mathbf{r}}_2 \times \hat{\mathbf{p}}_2, \frac{1}{|\hat{\mathbf{r}}_1 - \hat{\mathbf{r}}_2|} \right] = 0. \quad (\text{A26})$$

Hence, the second term in Eq. (A25) is also zero. Hence, we have proven Eq. (A5).

APPENDIX B: CARTESIAN COORDINATES IN BOHR

1. Equilibrium geometries

The equilibrium geometries for the molecules investigated in Tables I–VI were optimized with restricted Hartree–Fock and a cc-pVTZ basis set.

- H₂

| | | | |
|---|------------------------|-----------------------|-----------------------|
| H | -0.693 827 279 423 610 | 0.000 000 000 000 000 | 0.000 000 000 000 000 |
| H | 0.693 827 279 423 610 | 0.000 000 000 000 000 | 0.000 000 000 000 000 |

- LiH

| | | | |
|----|------------------------|-----------------------|-----------------------|
| Li | -0.381 507 444 748 606 | 0.000 000 000 000 000 | 0.000 000 000 000 000 |
| H | 2.655 860 841 963 647 | 0.000 000 000 000 000 | 0.000 000 000 000 000 |

- HCN

| | | | |
|---|------------------------|-----------------------|-----------------------|
| H | -3.023 887 918 951 979 | 0.000 000 000 000 000 | 0.000 000 000 000 000 |
| C | -1.027 314 918 951 979 | 0.000 000 000 000 000 | 0.000 000 000 000 000 |
| N | 1.097 998 081 048 021 | 0.000 000 000 000 000 | 0.000 000 000 000 000 |

- H₂O

| | | | |
|---|------------------------|------------------------|-----------------------|
| H | 1.777 459 680 682 990 | 0.000 000 000 000 000 | 0.000 000 000 000 000 |
| O | 0.000 000 000 000 000 | 0.000 000 000 000 000 | 0.000 000 000 000 000 |
| H | -0.489 811 956 048 840 | -1.708 638 980 055 550 | 0.000 000 000 000 000 |

- C₄H₂

| | | | |
|---|------------------------|-----------------------|-----------------------|
| H | -5.534 109 801 000 000 | 0.000 000 000 000 000 | 0.000 000 000 000 000 |
| C | -3.542 659 862 000 000 | 0.000 000 000 000 000 | 0.000 000 000 000 000 |
| C | -1.308 625 798 000 000 | 0.000 000 000 000 000 | 0.000 000 000 000 000 |
| C | 1.308 625 798 000 000 | 0.000 000 000 000 000 | 0.000 000 000 000 000 |
| C | 3.542 659 862 000 000 | 0.000 000 000 000 000 | 0.000 000 000 000 000 |
| H | 5.534 109 801 000 000 | 0.000 000 000 000 000 | 0.000 000 000 000 000 |

2. LiH dimer

| | | | |
|----|------------------------|------------------------|-----------------------|
| Li | -0.381 507 444 748 606 | 0.000 000 000 000 000 | 0.000 000 000 000 000 |
| H | 2.655 860 841 963 647 | 0.000 000 000 000 000 | 0.000 000 000 000 000 |
| Li | 35.000 000 000 000 00 | -0.381 507 444 748 606 | 0.000 000 000 000 000 |
| H | 35.000 000 000 000 00 | 2.655 860 841 963 647 | 0.000 000 000 000 000 |

TABLE V. The electronic linear momentum (\hbar/a_0) calculated with the phase-space Hamiltonian approach with two choices of Γ : the electron translation factor (Γ') and the electron rotation factor (Γ''). The velocity used here corresponds to stretching one H atom along the x axis of the water molecule.

| | STO-3G | DZ | aDZ | TZ | aTZ | QZ | aQZ |
|-------------------------------|------------|-----------------------|------------------------|------------------------|------------------------|------------------------|------------------------|
| $\langle \hat{p}_e^x \rangle$ | Γ' | 3.57×10^{-4} | 7.11×10^{-4} | 6.67×10^{-4} | 2.75×10^{-4} | 5.13×10^{-4} | 2.03×10^{-4} |
| | Γ'' | 1.21×10^{-5} | 4.18×10^{-5} | -9.90×10^{-6} | 6.20×10^{-5} | -1.52×10^{-6} | 7.40×10^{-5} |
| $\langle \hat{p}_e^y \rangle$ | Γ' | 5.82×10^{-6} | -6.86×10^{-5} | -4.20×10^{-5} | -1.08×10^{-4} | -1.21×10^{-5} | -1.96×10^{-4} |
| | Γ'' | 9.15×10^{-6} | 3.15×10^{-5} | -7.46×10^{-6} | 4.67×10^{-5} | -1.17×10^{-6} | -5.57×10^{-5} |

TABLE VI. The electronic angular momentum (\hat{L}_e) (\hbar) calculated with the phase-space Hamiltonian approach with the electron translation factor (Γ') or the electron rotation factor (Γ'') only. The velocity used here corresponds to a rigid rotation around the z axis of the linear molecules aligned at the x axis.

| | STO-3G | DZ | aDZ | TZ | aTZ | QZ | aQZ |
|-------------------------------|------------|-----------------------|------------------------|------------------------|------------------------|------------------------|------------------------|
| H ₂ | Γ' | 0.00 | 1.37×10^{-4} | 3.26×10^{-4} | 2.40×10^{-4} | 2.47×10^{-4} | 2.88×10^{-4} |
| | Γ'' | 0.00 | -8.40×10^{-5} | -2.51×10^{-5} | -1.68×10^{-4} | -1.75×10^{-4} | -2.15×10^{-4} |
| Stretched H ₂ | Γ' | 0.00 | 6.93×10^{-3} | 2.33×10^{-2} | 1.35×10^{-2} | 2.46×10^{-2} | 1.72×10^{-2} |
| | Γ'' | 0.00 | -1.70×10^{-5} | -6.68×10^{-4} | -9.67×10^{-5} | -9.85×10^{-4} | -2.02×10^{-4} |
| LiH | Γ' | 9.11×10^{-4} | 3.50×10^{-3} | 6.22×10^{-3} | 4.93×10^{-3} | 7.55×10^{-3} | 5.77×10^{-3} |
| | Γ'' | 4.83×10^{-3} | 5.89×10^{-3} | 4.47×10^{-3} | 5.73×10^{-3} | 3.64×10^{-3} | 5.34×10^{-3} |
| HCN | Γ' | 3.33×10^{-4} | 1.96×10^{-3} | 2.41×10^{-3} | 2.71×10^{-3} | 2.66×10^{-3} | 2.98×10^{-3} |
| | Γ'' | 2.14×10^{-3} | 1.53×10^{-3} | 1.28×10^{-3} | 1.27×10^{-3} | 1.40×10^{-3} | 1.27×10^{-3} |
| C ₄ H ₂ | Γ' | 5.78×10^{-4} | 8.17×10^{-3} | 1.18×10^{-2} | 9.74×10^{-3} | 9.76×10^{-3} | 1.07×10^{-2} |
| | Γ'' | 9.60×10^{-4} | -6.76×10^{-4} | -2.97×10^{-3} | -2.90×10^{-5} | 5.58×10^{-4} | 2.40×10^{-4} |

APPENDIX C: ETF AND ERF CONTRIBUTIONS

1. Linear momentum when stretching an H atom of a water molecule

For all the molecules studied in Table II, the contributions of Γ'' are non-zero only for the water molecule. In Table V, we show the linear momentum as calculated with either Γ' or Γ'' exclusively. Here, the water molecule is placed in the xy plane with one of the O–H bonds aligned along the x axis. Moving the H atom away from the O atom along the x axis puts the majority of the linear momentum in the x direction ($\langle \hat{p}_e^x \rangle$) and a small degree in the y direction ($\langle \hat{p}_e^y \rangle$). Comparing the contributions from the two components of the Γ coupling (Γ' vs Γ''), we note that the contribution from Γ'' to the linear momentum is much smaller (by an order of magnitude) as compared to the contribution from Γ' .

2. Angular momentum of rigid rotations of linear molecules

In this section, we provide data regarding the angular momentum as calculated using either Γ' and Γ'' exclusively. As shown in Table VI, depending on the molecules, for the equilibrium geometries, the angular momentum calculated with only Γ'' can be the same magnitude or one magnitude smaller than what is found when using Γ' alone. At the geometry for which the diatomic bond lengths are stretched to 8 bohrs, the contribution from Γ' clearly dominates the contribution from Γ'' .

REFERENCES

- M. Born and R. Oppenheimer, “Zur Quantentheorie der Moleküle,” *Ann. Phys.* **389**, 457–484 (1927).
- J. C. Tully, “Perspective on ‘Zur Quantentheorie der Moleküle’,” *Theor. Chem. Acc.* **103**, 173–176 (2000).
- M. Barbatti, “Nonadiabatic dynamics with trajectory surface hopping method,” *Wiley Interdiscip. Rev.: Comput. Mol. Sci.* **1**, 620–633 (2011).
- B. F. E. Curchod, U. Rothlisberger, and I. Tavernelli, “Trajectory-Based nonadiabatic dynamics with time-dependent density functional theory,” *ChemPhysChem* **14**, 1314–1340 (2013).
- E. Tapavicza, G. D. Bellchambers, J. C. Vincent, and F. Furche, “*Ab initio* non-adiabatic molecular dynamics,” *Phys. Chem. Chem. Phys.* **15**, 18336–18348 (2013).
- T. Nelson, S. Fernandez-Alberti, A. E. Roitberg, and S. Tretiak, “Nonadiabatic excited-state molecular dynamics: Modeling photophysics in organic conjugated materials,” *Acc. Chem. Res.* **47**, 1155–1164 (2014).
- X. Bian, Z. Tao, Y. Wu, J. Rawlinson, R. G. Littlejohn, and J. E. Subotnik, “Total angular momentum conservation in ab initio Born–Oppenheimer molecular dynamics,” *Phys. Rev. B* **108**, L220304 (2023).
- R. Littlejohn, J. Rawlinson, and J. Subotnik, “Representation and conservation of angular momentum in the Born–Oppenheimer theory of polyatomic molecules,” *J. Chem. Phys.* **158**, 104302 (2023).
- C. A. Mead, “The “noncrossing” rule for electronic potential energy surfaces: The role of time-reversal invariance,” *J. Chem. Phys.* **70**, 2276–2283 (1979).
- T. Culpitt, L. D. M. Peters, E. I. Tellgren, and T. Helgaker, “Analytic calculation of the Berry curvature and diagonal Born–Oppenheimer correction for molecular systems in uniform magnetic fields,” *J. Chem. Phys.* **156**, 044121 (2022).
- Z. Tao, T. Qiu, and J. E. Subotnik, “Symmetric post-transition state bifurcation reactions with Berry pseudomagnetic fields,” *J. Phys. Chem. Lett.* **14**, 770–778 (2023).

- ¹²Z. Tao, X. Bian, Y. Wu, J. Rawlinson, R. G. Littlejohn, and J. E. Subotnik, "Total angular momentum conservation in Ehrenfest dynamics with a truncated basis of adiabatic states," *J. Chem. Phys.* **160**, 054104 (2024).
- ¹³M. Amano and K. Takatsuka, "Quantum fluctuation of electronic wave-packet dynamics coupled with classical nuclear motions," *J. Chem. Phys.* **122**, 084113 (2005).
- ¹⁴V. Krishna, "Path integral formulation for quantum nonadiabatic dynamics and the mixed quantum classical limit," *J. Chem. Phys.* **126**, 134107 (2007).
- ¹⁵C. A. Mead, "The geometric phase in molecular systems," *Rev. Mod. Phys.* **64**, 51–85 (1992).
- ¹⁶Y. Wu, J. Rawlinson, R. G. Littlejohn, and J. E. Subotnik, "Linear and angular momentum conservation in surface hopping methods," *J. Chem. Phys.* **160**, 024119 (2024).
- ¹⁷N. Shenvi, "Phase-space surface hopping: Nonadiabatic dynamics in a superadiabatic basis," *J. Chem. Phys.* **130**, 124117 (2009).
- ¹⁸R. Gherib, L. Ye, I. G. Ryabinkin, and A. F. Izmaylov, "On the inclusion of the diagonal Born–Oppenheimer correction in surface hopping methods," *J. Chem. Phys.* **144**, 154103 (2016).
- ¹⁹L. A. Nafie, "Adiabatic molecular properties beyond the Born–Oppenheimer approximation. Complete adiabatic wave functions and vibrationally induced electronic current density," *J. Chem. Phys.* **79**, 4950–4957 (1983).
- ²⁰L. A. Nafie, "Velocity-gauge formalism in the theory of vibrational circular dichroism and infrared absorption," *J. Chem. Phys.* **96**, 5687–5702 (1992).
- ²¹L. A. Nafie, "Infrared and Raman vibrational optical activity: Theoretical and experimental aspects," *Annu. Rev. Phys. Chem.* **48**, 357–386 (1997).
- ²²L. A. Nafie, "Theory of vibrational circular dichroism and infrared absorption: Extension to molecules with low-lying excited electronic states," *J. Phys. Chem. A* **108**, 7222–7231 (2004).
- ²³E. Wigner, "On a modification of the Rayleigh–Schrödinger perturbation theory," *Math. Natur. Anz. (Budapest)* **53**, 477–482 (1935).
- ²⁴J. G. Ángyán, "Wigner's $(2n + 1)$ rule for nonlinear Schrödinger equations," *J. Math. Chem.* **46**, 1–14 (2009).
- ²⁵T. Qiu, M. Bhati, Z. Tao, X. Bian, J. Rawlinson, R. G. Littlejohn, and J. E. Subotnik, "A simple expression for electron rotational factors," *J. Chem. Phys.* **160**, 124102 (2009).
- ²⁶J. C. Tully, "Molecular dynamics with electronic transitions," *J. Chem. Phys.* **93**, 1061–1071 (1990).
- ²⁷T. Nelson, S. Fernandez-Alberti, V. Chernyak, A. E. Roitberg, and S. Tretyak, "Nonadiabatic excited-state molecular dynamics modeling of photoinduced dynamics in conjugated molecules," *J. Phys. Chem. B* **115**, 5402–5414 (2011).
- ²⁸L. Wang, A. Akimov, and O. V. Prezhdo, "Recent progress in surface hopping: 2011–2015," *J. Phys. Chem. Lett.* **7**, 2100–2112 (2016).
- ²⁹F. Fatehi, E. Alguire, Y. Shao, and J. E. Subotnik, "Analytic derivative couplings between configuration-interaction-singles states with built-in electron-translation factors for translational invariance," *J. Chem. Phys.* **135**, 234105 (2011).
- ³⁰V. Athavale, X. Bian, Z. Tao, Y. Wu, T. Qiu, J. Rawlinson, R. G. Littlejohn, and J. E. Subotnik, "Surface hopping, electron translation factors, electron rotation factors, momentum conservation, and size consistency," *J. Chem. Phys.* **159**, 114120 (2023).
- ³¹P. Pechukas, "Time-dependent semiclassical scattering theory. II. Atomic collisions," *Phys. Rev.* **181**, 174–185 (1969).
- ³²M. F. Herman, "Nonadiabatic semiclassical scattering. I. Analysis of generalized surface hopping procedures," *J. Chem. Phys.* **81**, 754–763 (1984).
- ³³R. Kapral and G. Ciccotti, "Mixed quantum-classical dynamics," *J. Chem. Phys.* **110**, 8919–8929 (1999).
- ³⁴J. E. Subotnik, W. Ouyang, and B. R. Landry, "Can we derive Tully's surface-hopping algorithm from the semiclassical quantum Liouville equation: Almost, but only with decoherence," *J. Chem. Phys.* **139**, 214107 (2013).
- ³⁵Y. Shu, L. Zhang, Z. Varga, K. A. Parker, S. Kanchanakungwankul, S. Sun, and D. G. Truhlar, "Conservation of angular momentum in direct nonadiabatic dynamics," *J. Phys. Chem. Lett.* **11**, 1135–1140 (2020).
- ³⁶D. R. Bates and R. McCarroll, "Electron capture in slow collisions," *Proc. R. Soc. London, Ser. A* **245**, 175–183 (1958).
- ³⁷S. B. Schneiderman and A. Russek, "Velocity-dependent orbitals in proton-on-hydrogen-atom collisions," *Phys. Rev.* **181**, 311–321 (1969).
- ³⁸W. R. Thorson and J. B. Delos, "Theory of near-adiabatic collisions. I. Electron translation factor method," *Phys. Rev. A* **18**, 117–134 (1978).
- ³⁹J. B. Delos, "Theory of electronic transitions in slow atomic collisions," *Rev. Mod. Phys.* **53**, 287–357 (1981).
- ⁴⁰E. Deumens, A. Diz, R. Longo, and Y. Öhrn, "Time-dependent theoretical treatments of the dynamics of electrons and nuclei in molecular systems," *Rev. Mod. Phys.* **66**, 917–983 (1994).
- ⁴¹L. F. Errea, C. Harel, H. Jouini, L. Mendez, B. Pons, and A. Riera, "Common translation factor method," *J. Phys. B: At., Mol. Opt. Phys.* **27**, 3603 (1994).
- ⁴²C. Illescas and A. Riera, "Classical outlook on the electron translation factor problem," *Phys. Rev. Lett.* **80**, 3029–3032 (1998).
- ⁴³B. H. Lengsfeld, P. Saxe, and D. R. Yarkony, "On the evaluation of nonadiabatic coupling matrix elements using SA-MCSCF/CI wave functions and analytic gradient methods. I," *J. Chem. Phys.* **81**, 4549–4553 (1984).
- ⁴⁴P. Saxe, B. H. Lengsfeld, and D. R. Yarkony, "On the evaluation of nonadiabatic coupling matrix elements for large scale CI wavefunctions," *Chem. Phys. Lett.* **113**, 159–164 (1985).
- ⁴⁵H. Lisicka, M. Dallos, P. G. Szalay, D. R. Yarkony, and R. Shepard, "Analytic evaluation of nonadiabatic coupling terms at the MR-CI level. I. Formalism," *J. Chem. Phys.* **120**, 7322–7329 (2004).
- ⁴⁶V. Chernyak and S. Mukamel, "Density-matrix representation of nonadiabatic couplings in time-dependent density functional (TDDFT) theories," *J. Chem. Phys.* **112**, 3572–3579 (2000).
- ⁴⁷R. Send and F. Furche, "First-order nonadiabatic couplings from time-dependent hybrid density functional response theory: Consistent formalism, implementation, and performance," *J. Chem. Phys.* **132**, 044107 (2010).
- ⁴⁸I. Tavernelli, B. F. E. Curchod, A. Laktionov, and U. Rothlisberger, "Nonadiabatic coupling vectors for excited states within time-dependent density functional theory in the Tamm–Dancoff approximation and beyond," *J. Chem. Phys.* **133**, 194104 (2010).
- ⁴⁹Q. Ou, E. Alguire, and J. E. Subotnik, "Derivative couplings between time-dependent density functional theory excited states in the random-phase approximation based on pseudo-wavefunctions: Behavior around conical intersections," *J. Phys. Chem. B* **119**, 7150–7161 (2015).
- ⁵⁰E. Alguire, Q. Ou, and J. E. Subotnik, "Calculating derivative couplings between time-dependent Hartree–Fock excited states with pseudo-wavefunctions," *J. Phys. Chem. B* **119**, 7140–7149 (2015).
- ⁵¹Q. Ou, G. D. Bellchambers, F. Furche, and J. E. Subotnik, "First-order derivative couplings between excited states from adiabatic TDDFT response theory," *J. Chem. Phys.* **142**, 064114 (2015).
- ⁵²X. Zhang and J. M. Herbert, "Analytic derivative couplings for spin-flip configuration interaction singles and spin-flip time-dependent density functional theory," *J. Chem. Phys.* **141**, 064104 (2014).
- ⁵³D. J. Diestler, "Coupled-channels quantum theory of electronic flux density in electronically adiabatic processes: Fundamentals," *J. Phys. Chem. A* **116**, 2728–2735 (2012).
- ⁵⁴D. J. Diestler, "Quasi-classical theory of electronic flux density in electronically adiabatic molecular processes," *J. Phys. Chem. A* **116**, 11161–11166 (2012).
- ⁵⁵D. J. Diestler, A. Kenfack, J. Manz, B. Paulus, J. F. Pérez-Torres, and V. Pohl, "Computation of the electronic flux density in the Born–Oppenheimer approximation," *J. Phys. Chem. A* **117**, 8519–8527 (2013).
- ⁵⁶T. Bredtmann, D. J. Diestler, S.-D. Li, J. Manz, J. F. Pérez-Torres, W.-J. Tian, Y.-B. Wu, Y. Yang, and H.-J. Zhai, "Quantum theory of concerted electronic and nuclear fluxes associated with adiabatic intramolecular processes," *Phys. Chem. Chem. Phys.* **17**, 29421–29464 (2015).
- ⁵⁷W. Kutzelnigg, "Which masses are vibrating or rotating in a molecule?," *Mol. Phys.* **105**, 2627–2647 (2007).
- ⁵⁸K. Nagashima and K. Takatsuka, "Electron-wavepacket reaction dynamics in proton transfer of formamide," *J. Phys. Chem. A* **113**, 15240–15249 (2009).
- ⁵⁹M. Okuyama and K. Takatsuka, "Electron flux in molecules induced by nuclear motion," *Chem. Phys. Lett.* **476**, 109–115 (2009).
- ⁶⁰S. Patchkovskii, "Electronic currents and Born–Oppenheimer molecular dynamics," *J. Chem. Phys.* **137**, 084109 (2012).
- ⁶¹D. J. Diestler, "Beyond the Born–Oppenheimer approximation: A treatment of electronic flux density in electronically adiabatic molecular processes," *J. Phys. Chem. A* **117**, 4698–4708 (2013).

- ⁶²A. Schild, F. Agostini, and E. K. U. Gross, "Electronic flux density beyond the Born–Oppenheimer approximation," *J. Phys. Chem. A* **120**, 3316–3325 (2016).
- ⁶³T. Schaupp, J. Albert, and V. Engel, "Time-dependent electron momenta from Born–Oppenheimer calculations," *Eur. Phys. J. B* **91**, 97 (2018).
- ⁶⁴T. Schaupp and V. Engel, "On the calculation of time-dependent electron momenta within the Born–Oppenheimer approximation," *J. Chem. Phys.* **150**, 164110 (2019).
- ⁶⁵T. Schaupp and V. Engel, "Born–Oppenheimer and non-Born–Oppenheimer contributions to time-dependent electron momenta," *J. Chem. Phys.* **152**, 204310 (2020).
- ⁶⁶T. Schaupp and V. Engel, "Quantum flux densities for electronic–nuclear motion: Exact versus Born–Oppenheimer dynamics," *Philos. Trans. R. Soc., A* **380**, 20200385 (2022).
- ⁶⁷K. Hanasaki and K. Takatsuka, "On the molecular electronic flux: Role of nonadiabaticity and violation of conservation," *J. Chem. Phys.* **154**, 164112 (2021).
- ⁶⁸V. Pohl and J. C. Tremblay, "Adiabatic electronic flux density: A Born–Oppenheimer broken-symmetry ansatz," *Phys. Rev. A* **93**, 012504 (2016).
- ⁶⁹H. Nakamura and M. Namiki, "Non-adiabatic transitions induced by rotational coupling," *J. Phys. Soc. Jpn.* **49**, 843–844 (1980).
- ⁷⁰C. Li, R. Requist, and E. K. U. Gross, "Energy, momentum, and angular momentum transfer between electrons and nuclei," *Phys. Rev. Lett.* **128**, 113001 (2022).
- ⁷¹A. Abedi, N. T. Maitra, and E. K. U. Gross, "Exact factorization of the time-dependent electron-nuclear wave function," *Phys. Rev. Lett.* **105**, 123002 (2010).
- ⁷²A. Abedi, N. T. Maitra, and E. K. U. Gross, "Correlated electron-nuclear dynamics: Exact factorization of the molecular wavefunction," *J. Chem. Phys.* **137**, 22A530 (2012).
- ⁷³R. Requist and E. K. U. Gross, "Exact factorization-based density functional theory of electrons and nuclei," *Phys. Rev. Lett.* **117**, 193001 (2016).
- ⁷⁴P. J. Stephens and M. A. Lowe, "Vibrational circular dichroism," *Annu. Rev. Phys. Chem.* **36**, 213–241 (1985).
- ⁷⁵L. A. Nafie, R. K. Dukor, and T. B. Freedman, in *Handbook of Vibrational Spectroscopy* (Wiley, 2001).
- ⁷⁶G. Magyarlalvi, G. Tarczay, and E. Vass, "Vibrational circular dichroism," *Wiley Interdiscip. Rev.: Comput. Mol. Sci.* **1**, 403–425 (2011).
- ⁷⁷L. A. Nafie, "Vibrational optical activity: From discovery and development to future challenges," *Chirality* **32**, 667–692 (2020).
- ⁷⁸L. A. Nafie and T. H. Walnut, "Vibrational circular dichroism theory: A localized molecular orbital model," *Chem. Phys. Lett.* **49**, 441–446 (1977).
- ⁷⁹L. A. Nafie and T. B. Freedman, "Vibronic coupling theory of infrared vibrational transitions," *J. Chem. Phys.* **78**, 7108–7116 (1983).
- ⁸⁰D. P. Craig and T. Thirunamachandran, "A theory of vibrational circular dichroism in terms of vibronic interactions," *Mol. Phys.* **35**, 825–840 (1978).
- ⁸¹D. P. Craig and T. Thirunamachandran, "The adiabatic approximation in the ground-state manifold," *Can. J. Chem.* **63**, 1773–1779 (1985).
- ⁸²P. J. Stephens, "Theory of vibrational circular dichroism," *J. Phys. Chem.* **89**, 748–752 (1985).
- ⁸³P. J. Stephens, "Gauge dependence of vibrational magnetic dipole transition moments and rotational strengths," *J. Phys. Chem.* **91**, 1712–1715 (1987).
- ⁸⁴A. D. Buckingham, P. W. Fowler, and P. A. Galwas, "Velocity-dependent property surfaces and the theory of vibrational circular dichroism," *Chem. Phys.* **112**, 1–14 (1987).
- ⁸⁵D. Yang and A. Rauk, "Vibrational circular dichroism intensities: *Ab initio* vibronic coupling theory using the distributed origin gauge," *J. Chem. Phys.* **97**, 6517–6534 (1992).
- ⁸⁶A. Scherrer, F. Agostini, D. Sebastiani, E. K. U. Gross, and R. Vuilleumier, "Nuclear velocity perturbation theory for vibrational circular dichroism: An approach based on the exact factorization of the electron-nuclear wave function," *J. Chem. Phys.* **143**, 074106 (2015).
- ⁸⁷A. Scherrer, R. Vuilleumier, and D. Sebastiani, "Nuclear velocity perturbation theory of vibrational circular dichroism," *J. Chem. Theory Comput.* **9**, 5305–5312 (2013).
- ⁸⁸A. Scherrer, R. Vuilleumier, and D. Sebastiani, "Vibrational circular dichroism from *ab initio* molecular dynamics and nuclear velocity perturbation theory in the liquid phase," *J. Chem. Phys.* **145**, 084101 (2016).
- ⁸⁹E. Ditler, T. Zimmermann, C. Kumar, and S. Luber, "Implementation of nuclear velocity perturbation and magnetic field perturbation theory in CP2K and their application to vibrational circular dichroism," *J. Chem. Theory Comput.* **18**, 2448–2461 (2022).
- ⁹⁰As a side note, we mention that the ETFs described in the present paper correspond exactly to velocity-gauge factors in the NVP literature, but there is no analog to ERFs in the latter.
- ⁹¹R. Naaman and D. H. Waldeck, "Chiral-induced spin selectivity effect," *J. Phys. Chem. Lett.* **3**, 2178–2187 (2012).
- ⁹²R. Naaman, Y. Paltiel, and D. H. Waldeck, "Chiral molecules and the electron spin," *Nat. Rev. Chem.* **3**, 250–260 (2019).
- ⁹³F. Evers, A. Aharony, N. Bar-Gill, O. Entin-Wohlman, P. Hedegård, O. Hod, P. Jelinek, G. Kamieniarz, M. Lemeshko, K. Michaeli, V. Mujica, R. Naaman, Y. Paltiel, S. Refaelly-Abramson, O. Tal, J. Thijssen, M. Thoss, J. M. van Ruitenbeek, L. Venkataraman, D. H. Waldeck, B. Yan, and L. Kronik, "Theory of chirality induced spin selectivity: Progress and challenges," *Adv. Mater.* **34**, 2106629 (2022).
- ⁹⁴T. K. Das, F. Tassinari, R. Naaman, and J. Fransson, "Temperature-dependent chiral-induced spin selectivity effect: Experiments and theory," *J. Phys. Chem. C* **126**, 3257–3264 (2022).
- ⁹⁵J. Fransson, "Chiral phonon induced spin polarization," *Phys. Rev. Res.* **5**, L022039 (2023).
- ⁹⁶L. Hall, A. Armstrong, W. Moonaw, and M. A. El-Sayed, "Spin-lattice relaxation and the decay of pyrazine phosphorescence at low temperatures," *J. Chem. Phys.* **48**, 1395–1396 (1968).
- ⁹⁷M. A. El-Sayed, "Proposed method for determining all the rate constants of processes involving the lowest triplet state at low temperature," *J. Chem. Phys.* **52**, 6438–6440 (1970).
- ⁹⁸L. H. Hall and M. A. El-Sayed, "Optical determination of the electron spin-lattice relaxation mechanisms between the zero-field levels of the lowest triplet state," *J. Chem. Phys.* **54**, 4958–4959 (1971).
- ⁹⁹L. H. Hall and M. A. El-Sayed, "Magnetic field dependence of spin-lattice relaxation rates between the triplet state Zeeman levels of pyrazine-*d*₄ at 1-K," *Mol. Phys.* **22**, 361–364 (1971).
- ¹⁰⁰L. H. Hall and M. A. El-Sayed, "Temperature dependence of the spin-lattice relaxation rates in the triplet state of pyrazine at low temperatures," *Chem. Phys.* **8**, 272–288 (1975).
- ¹⁰¹U. E. Steiner and T. Ulrich, "Magnetic field effects in chemical kinetics and related phenomena," *Chem. Rev.* **89**, 51–147 (1989).
- ¹⁰²J. M. D. Coey, *Magnetism and Magnetic Materials* (Cambridge University Press, Cambridge, 2010).
- ¹⁰³T. Helgaker, S. Coriani, P. Jørgensen, K. Kristensen, J. Olsen, and K. Ruud, "Recent advances in wave function-based methods of molecular-property calculations," *Chem. Rev.* **112**, 543–631 (2012).
- ¹⁰⁴R. A. Marcus and N. Sutin, "Electron transfers in chemistry and biology," *Biochim. Biophys. Acta, Rev. Bioenerg.* **811**, 265–322 (1985).
- ¹⁰⁵A. Nitzan, *Chemical Dynamics in Condensed Phases* (Oxford University Press, 2006).